Giant, 11, 2022, 100103

Full-length article

Molecular parameters including fluorination program order during hierarchical helical self-organization of self-assembling dendrons

Mihai Peterca, Mohammad R. Imam, Andres E. Dulcey, Kentaro Morimitsu, Qi Xiao, Devendra S. Maurya, Virgil Percec*

Roy & Diana Vagelos Laboratories, Department of Chemistry, University of Pennsylvania, Philadelphia, Pennsylvania 19104-6323, United States

Keywords: Hierarchical, Self-organization, Self-assembly, Fluorinated helical porous columns, Spherical helix, Frank-Kasper A15

Primary structure endows tertiary structure while tertiary structure determines function. This fundamental principle is responsible for the generation of high order and precise functions in both biological assemblies including giant and mega proteins and nucleic acids as well as in metals generated from only few atoms. However, this size-independent ability to generate high order and very precise functions is not yet accessible in non-biological assemblies that use the same principles for their hierarchical self-organization. Here we report a study investigating the role of the molecular parameters on the hierarchical self-organizations of helical columnar assemblies produced from the column-forming self-assembling dendron (4-3,4-3,5)-X with a linear or branched hydrogenated or linear semifluorinated alkyl groups while apex is -CO_2CH_3 or -CH_2OH. A combination of differential scanning calorimetry, small and wide-angle powder and oriented fiber X-ray diffraction experiments together with helical diffraction theory, 2-D and 3-D electron density maps were employed in these structural analysis experiments. They demonstrated that H-bonding at the apex of the self-assembling dendron enhanced the order of the helical columns by comparison with the order of supramolecular helical columns based on dendrons containing an ester group at their apex. This was the case for both linear and branched alkyl groups at the periphery of the self-assembling dendron. Unexpectedly, self-assembling dendrons containing semifluorinated alkyl groups on their periphery and H-bonding groups at their apex increase even more the order of their supramolecular perfluorinated porous helical column. In all cases helix is mediated by the aromatic part of the dendron but hierarchically influenced both by the apex and peripheral groups. A combination of branched alkyl groups with H-bonding at the apex produced a new mechanism to transform helical columns assembled from the column-forming (4-3,4-3,5)-X self-assembling dendron into spherical assemblies, organized from conical dendron conformers, forming an A15 Frank-Kasper phase.

* Corresponding authors.
E-mail address: percec@sas.upenn.edu (V. Percec).
Received 27 April 2022; Received in revised form 5 May 2022; Accepted 6 May 2022

https://doi.org/10.1016/j.giant.2022.100103

Introduction

Columnar assemblies were first self-organized from disc-like molecules [1–3] and even from conformationally flexible disc-like molecules such as CTTV [4–8], subsequently from crown-like molecules [9–12], phasmids and polycatenar building blocks [13] and almost simultaneously from self-assembling dendrons and self-organizable dendronized polymers [14–36]. Dendrons represent a fragment of a disc-like molecule or of a crown-like conformation. The history of the discovery of self-assembling dendrons and self-organizable dendronized polymers by using tobacco mosaic virus, TMV, as inspiration was reported [36–47]. The nomenclature employed in this report was defined previously [43] and it will be only briefly mentioned here for self-assembly and self-organization. For additional definitions the readers are encouraged to consult reference [43]. Self-assembly refers to the process by which certain building blocks, like specifically designed dendrons or dendrimers, aggregate to form supramolecular objects. Not all dendrons and dendrimers self-assembleo0. Self-organization is the process by which supramolecular or macromolecular objects arrange themselves into periodic or quasiperiodic arrays in solid state or solution. Columnar self-organizations were also discovered and designed from much-simpler non-disc-like molecules such us main-chain liquid crystal polyethers [48–54] and copolyethers [55–59]. However, the largest diversity of functions is accessible from supramolecular columns assembled from self-assembling dendrons or self-organizable dendronized polymers. Ionic [25] and electronic conductivity [60], water purification *via* aquaporin (AQP) channel mechanisms [61–71], new concepts to molecular machines [72–74], accelerated and self-interrupted organic reactions, polymerization and living polymerizations [75–79], transformation of a helix-coil into helix-helix transition [80], modification of organic reaction pathways and reaction mechanisms [80], programming order in supramolecular polymerization via chirality and origins of homochirality [67,68,81], homochiral columns by deracemization in the crystal state [82–85], fast switching liquid crystals [86], chiral supramolecular spheres and containers [11,12,87], chiral columns from chiral spheres [88], self-assembly via fluorous phase to generate perfluorinated objects from semifluorinated building blocks [60,73,79,89–98] are just few of the concepts elaborated with helical supramolecular columns self-organized from self-assembling dendrons. Last but not least, screening through rational libraries self-assembling dendrons and their self-organizable dendronized polymers [11,63,69,71,76–79,82–85,88,99–139] provided a transition, mediated *via* a large diversity of structural parameters, from columnar to globular or spherical supramolecular assemblies. Globular or spherical assemblies self-organize Frank-Kasper [77,108,119,126,128,129] and quasicrystal [135,136] phases and facilitated the transition from self-organization in bulk state to self-organization in organic solvents [82,83] and ultimately in water [140–166]. Numerous laboratories became involved in this topic of research [167–171]. This transition expanded the range of applications from those enumerated above for helical columnar assemblies to supramolecular orientational memory effect [172–178], mimics of biological membranes *via* Janus dendrimers and dendrimersomes [140–153,163], mimics of the cell membrane glycan *via* Janus glycodendrimers and glycodendrimersomes [142,154–162] and finally to the discovery of one-component sequence-defined ionizable amphiphilic Janus dendrimers (IAJDs) that provided a new methodology for the delivery of mRNA [164–166]. On the other way, soft Frank-Kasper and quasicrystal phases discovered with self-assembling dendrons have scattered through a large diversity of field of self-organized soft matter by being discovered in the meantime in block copolymers, lipids, DNA nanoparticles and many other classes of self-assembling building blocks [56–59,179–203]. The principle primary structure endows tertiary structure while tertiary structure provides the very precise functions of all these hierarchical self-organizations is valid for giant and even mega biological macromolecules such us proteins and nucleic acids [39,40,45,204] and for metal lattices produced only from a small number of atoms. These size-independent principles required to produce high order with very precise structures are, however, not yet fully elucidated in supramolecular assemblies. For example, in columnar assemblies obtained from disc-like molecules, high helical order was most probably observed first time by Ringsdorf [205] who also demonstrated the induction of their fast photoconductivity. After many years of investigations of covalent and supramolecular helical columns [23,31,32,33,206,207], it was the transplant of helical diffraction theory from biology to supramolecular assemblies [109] that facilitated access to the discovery of high helical order by deracemization in tapered dendron assemblies [82,83] and in cogwheel helical self-organizations *via* a sequence defined self-assembling dendron concept [83–85] as well as the elucidation of helical columns elaborated during the early days of self-organizable dendronized polymers [74]. These reports demanded the need for additional elucidation of primary structure-tertiary structure-function relationship in supramolecular assemblies. In this report we selected the column-forming self-assembling dendron (4-3,4-3,5)-X with a linear (*n*-hexyl, C_6H_{13}) or branched hydrogenated ((*S*)-3,7-dimethyloctyl, dm8*) or linear semifluorinated alkyl group ($(CH_2)_4(CF_2)_8F$, 12F8) while $-CO_2CH_3$ or $-CH_2OH$ in the apex to investigate the role of the primary structure of the self-assembling dendron on the helical self-organization of its supramolecular column. This self-assembling dendron is a classic column-forming building block employed in numerous investigations of dendritic dipeptides to elucidate the principles of self-assembly of AQP-like porous structures [61–71] that ultimately led to the most successful approach to water purification that is close to production on industrial scale [64,208,209]. The change from the dendritic dipeptide based on (4-3,4-3,5)-X to (4-3,4-3,4)-X where apex is dipeptide, transformed the helical porous supramolecular column into a hollow sphere capsule [69]. However, no other structural modification of the (4-3,4-3,5)-X dendritic dipeptide including the addition of branched alkyl groups on its periphery [99] could change the porous supramolecular column into a hollow supramolecular sphere. Semifluorinated alkyl groups were selected for these experiments since they were repeatedly employed by our laboratory to enhance the stability of the supramolecular columns and of other assemblies and generate perfluorinated columns from semifluorinated dendrons [60,73,79,89–98]. H-bonding units and other molecular recognition units at the apex of the dendrons

were also employed by our laboratory to mediate the stability of the supramolecular assemblies [25–29,111]. However, no single investigation combined the role of the H-bonding, branching, linear and semifluorinated alkyl groups into a single series of experiments. This combination of experiments will be reported in this publication.

Methods

Materials

Tetrahydrofuran (Fisher, ACS reagent grade) was refluxed over sodium/benzophenone and freshly distilled before use, dichloromethane (Fisher, ACS reagent grade) was refluxed over CaH_2 and freshly distilled before use. All other chemicals were commercially available and were used as received.

Techniques

Nuclear magnetic resonance (NMR) spectroscopy

^{1}H NMR (500 MHz), ^{13}C NMR (126 MHz), ^{19}F NMR (471 MHz) spectra were recorded on a Bruker DRX 500 instrument at 300K or other temperature indicated. Chemical shifts (δ) are reported in ppm and coupling constants (J) are reported in Hertz (Hz). The resonance multiplicities in the ^{1}H NMR spectra are described as "s" (singlet), "d" (doublet), "t" (triplet), "quint" (quintet) and "m" (multiplet) and broad resonances are indicated by "br". Residual protic solvent of $CDCl_3$ (^{1} H, δ 7.26 ppm; ^{13}C, δ 77.23 ppm, middle of the triplet), ^{19}F, δ –76.55 ppm from trifluoroacetic acid in $CDCl_3$ as external standard), and tetramethylsilane (TMS, δ 0 ppm) were also used as the internal reference in the ^{1}H and ^{13}C spectra.

Thin-layer chromatography (TLC) and high-pressure liquid chromatography (HPLC)

The purity of the products was determined by a combination of TLC on silica gel coated aluminum plates (with F_{254} indicator; layer thickness, 200 μm; particle size, 2-25 μm; pore size 60 Å, SIGMA-Aldrich) and HPLC using THF as mobile phase at 1 mL/min, on a Shimadzu LC-10AT high pressure liquid chromatograph equipped with a Perkin Elmer LC-100 oven (40 °C), containing two Perkin-Elmer PL gel columns of 5×10^2 and 1×10^4 Å, a Shimadzu SPD-10A UV detector (λ = 254 nm), a Shimadzu RID-10A RI-detector, and a PE Nelson Analytical 900 Series integrator data station.

Matrix-assisted laser desorption/ionization time-of-flight (MALDI-TOF)

MALDI-TOF mass spectrometry was performed on a PerSeptive Biosystems-Voyager-DE (Framingham, MA) mass spectrometer equipped with a nitrogen laser (337 nm) and operating in linear mode. Internal calibration was performed using Angiotensin II and Bombesin as standards. The analytical sample was obtained by mixing the THF solution of the sample (5-10 mg/ml) and THF solution of the matrix (3,5-dimethoxy-4-hydroxy-*trans*-cinnamic acid or 2,5-dihydroxyl benzoic acid 10 mg/mL) in a 1/5 v/v ratio. The prepared solution of the sample and the matrix (0.5 μL) was loaded on the MALDI-TOF plate and allowed to dry at 23°C before the plate was inserted into the vacuum chamber of the MALDI-TOF instrument. The laser steps and voltages applied were adjusted depending on both the molecular weight and the nature of each analyzed compound.

Differential scanning calorimeter (DSC)

Thermal transitions were determined on a TA Instruments Q100 DSC equipped with a refrigerated cooling system with 10°C•min^{-1} heating and cooling rates. Indium was used as calibration standard. The transition temperatures were calculated as the maxima and minima of their endothermic and exothermic peaks.

Thermal optical polarized microscopy (TOPM)

An Olympus BX51 optical microscope (100 X magnifications) equipped with a Mettler FP82HT hot stage and a Mettler Toledo FP90 Central Processor was used to verify thermal transitions and to characterize anisotropic textures.

Density measurements

Density (ρ_{20}) measurements were carried out by flotation in gradient columns at 20°C.

Melting points

Melting points were measured using a uni-melt capillary melting point apparatus (Arthur H. Thomas Company) and were uncorrected.

X-ray diffraction (XRD)

XRD measurements were performed using Cu-$K_{\alpha 1}$ radiation (α=1.54178 Å) from a Bruker-Nonius FR-591 rotating anode X-ray source equipped with a 0.2 × 0.2 mm^2 filament operated at 3.4 kW. The Cu radiation beam was collimated and focused by a single bent mirror and sagitally focused through a Si (111) monochromator, generating in a 0.3 × 0.4 mm^2 spot on a Bruker-AXS Hi-Star multiwire area detector. To minimize attenuation and background scattering, an integral vacuum was maintained along the length of the flight tube and within the sample chamber. Samples were held in quartz capillaries (0.7 – 1.0 mm in diameter), mounted in a temperature-controlled oven (temperature precision: ±0.1°C, temperature range from 120°C to 270°C). The distance between the sample and the detector was 12.0 cm for wide angles diffraction experiments and 54.0 cm for intermediate angles diffraction experiments respectively. Aligned samples for fiber XRD experiments were prepared using a custom-made extrusion device. [18] The powdered sample (~ 10 mg) was heated inside the extrusion device above isotropization temperature. After slow cooling from the isotropic phase, the fiber was extruded in the liquid crystal phase and cooled to 23°C. Typically, the aligned samples have a thickness of ~ 0.3-0.7 mm and a length of ~ 3-7 mm. All XRD measurements were done with the aligned sample axis perpendicular to the beam direction. XRD peaks position and intensity analysis was performed using Datasqueeze Software [210] (version 2.1) that allows background elimination and Gaussian, Lorentzian, Lorentzian squared, or Voigt peak-shape fitting. Molecular modeling calculations were done using the Materials Studio Modeling version 3.1 software from Accelrys. The package Discover module was used to perform the energy minimizations on the supramolecular structures with the following settings: PCFF or COMPASS force fields and Fletcher-Reeves algorithm for the conjugate gradient method. Cerius^2 package (Accelrys, version 3.8) was used for fiber XRD simulations.

Synthesis

The dendrons **14a** (4-3,4-3,5)6G2CO_2CH_3 and **15a** (4-3,4-3,5)6G2CH_2OH were synthesized, and characterized according to literature procedures [62,63,109]. The dendrons **14b** (4-3,4-3,5)dm8G2CO_2CH_3 and **15b** (4-3,4-3,5)dm8G2CH_2OH were synthesized, and characterized according to reported procedures [109]. The semifluorinated chain (**4c**) was synthesized, and characterized according to literature [48]. The benzyl chloride with a semifluorinated chain in 4 position (**8c**) was synthesized, and characterized according to literature [113].

Compound 10c: To a thoroughly degassed suspension of anhydrous K_2CO_3 (2.76 g, 20 mmol) in a mixture of DMF (40 mL) and THF (10 mL) was added methyl 3,4-dihydroxybenzoate (**9**) (0.84 g, 5.0 mol) and the reaction mixture was heated to 70°C. At that time **8c** was added (6.17 g, 10 mol) under Ar in small portions. After stirring for 12 h at 70°C, the reaction mixture was cooled to 23°C and poured into stirring ice/water (200 mL). The white granular solid was filtered and washed with H_2O and dried. The solid was dissolved in DCM/CFC-113 mixture and precipitated in methanol twice. The precipitate was filtered and dried under vacuum to obtain **10c** as a white solid (5.9 g, 89%). Purity (HPLC): 99+%; TLC (EtOAc/hexane = 3/7): Rf = 0.5. ^{1}H NMR (500 MHz, $CDCl_3$): δ = 7.62–7.65 (m, 2H, 2 × Ph*H*), 7.32–7.37 (m, 4H, 4 × Ph*H*), 6.86–6.94 (m, 5H, 5 × Ph*H*), 5.10–5.12 (m, 4H, 2 × CH_2Ph), 3.99–4.01 (m, 4H, 2 × CH_2OPh), 3.87 (s, 3H, CO_2CH_3), 2.13–2.20 (m, 4H, 2 × CF_2CH_2), 1.82–1.88 (m, 8H, 2 × $CF_2CH_2(CH_2)_2$). ^{13}C NMR (126 MHz, $CDCl_3$): δ = 167.01, 158.95, 158.90, 153.35, 148.73, 129.43, 129.19, 124.23, 123.37, 116.19, 114.77, 114.72, 113.82, 71.40, 71.00, 67.50, 52.14, 31.15, 30.97, 30.79, 28.97, 17.56. ^{19}F NMR (471 MHz, $CDCl_3$): δ = –81.23, –114.75, –122.07, –122.28, –123.08, –123.87, –126.48, –128.88, –133.75.

Compound 11c: To a slurry of $LiAlH_4$ (0.17 g, 4.5 mmol) in dry THF (50 mL) was cooled at 0°C, compound **10c** (4.0 g, 3.0 mmol) dissolved in dry THF (50 mL) was added dropwise. The reaction mixture was stirred at 23°C for 2 h and quenched with 1 mL of water, 1 mL of NaOH (15% in water), and then 3 mL of water. The mixture was filtered and dried over $MgSO_4$. After filtration, evaporation, and drying under vacuum **11c** was obtained as a white solid (3.8 g, 98%). Purity (HPLC): 99+%; TLC (EtOAc/hexane = 1/1): Rf = 0.5. ^{1}H NMR (500 MHz, $CDCl_3$): δ = 7.26–7.38 (m, 4H, 4 × Ph*H*), 6.98–7.00 (m, 2H, 2 × Ph*H*), 6.85–6.92 (m, 5H, 5 × Ph*H*), 5.06–5.11 (m, 4H, 2 × CH_2Ph), 4.58 (s, 2H, CH_2OH), 3.98–4.01 (m, 4H, 2 × CH_2OPh), 2.13–2.27 (m, 4H, 2 × CF_2CH_2), 1.82–1.88 (m, 8H, 2 × $CF_2CH_2(CH_2)_2$). ^{13}C NMR (126 MHz, $CDCl_3$): δ = 158.98, 158.96, 149.77, 149.08, 134.87, 130.01, 129.95, 129.53, 129.47, 120.60, 118.79, 115.99, 114.84, 114.82, 71.74, 71.56, 67.63, 65.63, 31.29, 31.11, 30.94, 30.73, 30.10, 29.13, 17.71. ^{19}F NMR (471 MHz, $CDCl_3$): δ = –81.06, –114.80, –122.10, –122.32, –123.12, –123.90, –126.49.

Compound 12c: To a stirring solution of compound **11c** (3.9 g, 3.0 mmol) and 2,6-di-*tert*-butylpyridine (DTBMP) (1.2 g, 6.0 mmol) in dry DCM (60 mL) and trifluorotoluene (40 mL), $SOCl_2$ (0.42 g, 3.6 mmol) were added under Ar and the solution was stirred for 0.5 h at 23°C. The solvent was removed by rotary evaporation and dried under vacuum. After recrystallization in acetone, the target compound **12c** was obtained as a which solid (3.6 g, 92 %). ^{1}H NMR (500 MHz, $CDCl_3$): δ = 7.26–7.36 (m, 4H, 4 × Ph*H*), 6.86–7.00 (m, 7H, 7 × Ph*H*), 5.06 (m, 4H, 2 × CH_2Ph), 4.51 (s, 2H, CH_2Cl), 3.98–4.01 (m, 4H, 2 × CH_2OPh), 2.12–2.22 (m, 4H, 2 × CF_2CH_2), 1.71–1.91 (m, 8H, 2 × $CF_2CH_2(CH_2)_2$). ^{13}C NMR (126 MHz, $CDCl_3$): δ = 158.87, 158.84, 149.59, 149.46, 130.96, 129.63, 129.60, 129.42, 129.26, 122.13, 118.61, 116.08, 115.38, 114.70, 111.35, 111.07, 75.04, 71.51, 71.40, 67.48, 66.92, 46.70, 37.65, 31.12, 30.95, 30.77, 30.20, 28.96, 17.54. ^{19}F NMR (471 MHz, $CDCl_3$): δ = –81.08, –114.77, –122.11, –122.32, –123.12, –123.91, –126.49.

Compound 14c, (4-3,4-3,5)12F8G2CO_2CH_3: To a thoroughly degassed suspension of anhydrous K_2CO_3 (0.69 g, 5.0 mmol) in DMF (50 mL) was added methyl 3,4-dihydroxybenzoate (**9**) (0.31 g, 1.25 mmol) and the reaction mixture was heated to 70°C. **12c** was added (3.3 g, 2.5 mol) under Ar in small portions. After stirring for 12 h at 70°C, the reaction mixture was cooled to 23°C and poured into stirring ice/water (200 mL). The white granular solid was filtered and washed with H_2O and dried. The solid was dissolved in THF, passed through a short column (basic alumina) and precipitated in acetone. The precipitate was filtered and dried under vacuum to obtain **14c** as a white solid (1.5 g, 44%). Purity (HPLC): 99+%; TLC (EtOAc/hexane = 3/7): Rf = 0. ^{1}H NMR (500 MHz, 40°C, $CDCl_3$): δ = 7.31–7.33 (m, 8H, 8 × Ph*H*), 7.25–7.28 (m, 2H, 2 × Ph*H*), 7.05 (s, 2H, 2 × Ph*H*), 6.93 (s, 4H, 4 × Ph*H*), 6.84–6.87 (m, 8H, 8 × Ph*H*), 6.75 (t, 1H, Ph*H*), 5.10–5.12 (m, 4H, 2 × CH_2Ph), 3.99–4.01 (m, 4H, 2 × CH_2OPh), 3.87 (s, 3H, CO_2CH_3), 2.13–2.20 (m, 4H, 2 × CF_2CH_2), 1.82–1.88 (m, 8H, 2 × $CF_2CH_2(CH_2)_2$). ^{13}C NMR (126 MHz, 40°C, $CDCl_3$): δ = 160.14, 158.92, 149.79, 149.53, 132.41, 130.24, 129.95, 129.87, 129.42, 129.32, 121.29, 115.98, 115.55, 114.79, 108.88, 107.73, 71.69, 70.56, 67.58, 52.37, 31.25, 31.07, 30.89, 29.04, 17.61. M.P. = 197°C, MALDI-TOF [M+K]+ *m/z*: calculated for $C_{98}H_{72}F_{68}KO_{12}$ 2771.4, observed 2771.9.

Compound 15c, (4-3,4-3,5)12F8G2CH_2OH: Compound **14c** (120 mg, 0.044 mmol) dissolved in dry THF (100 mL) and $LiAlH_4$ (20 mg, 0.05 mmol) was added slowly. The reaction mixture was stirred at 23°C for 2 h and quenched with 0.5 mL of saturated Na_2SO_4. The mixture was filtered, and the filtrate was dried over Na_2SO_4. After filtration, concentration with rotary evaporation, precipitation in methanol, filtration and drying under vacuum **15c** was obtained as a white solid (88 mg, 70%). Purity (HPLC): 99+%; MALDI-TOF $[M+K]^+$ *m/z*: calculated for $C_{97}H_{72}F_{68}KO_{11}$ 2743.4, observed 2743.6.

Results and discussion

Fig. 1 outlines the synthesis of (4-3,4-3,5)-X by combining methods elaborated in our laboratory to generate closely related dendritic dipeptides and other self-assembling building blocks [62,63].

$Pd(PPh_3)_4$ catalyzed cross-coupling reaction was used to cross-couple 3-butenoic acid (1) with n-$C_8F_{17}I$ in hexane at 0-20°C to produce 2 in 72% isolated yield. Reduction of 2 with $LiAlH_4$ in THF at 23 °C generated 2 in 2h reaction time. Bromination of 3 with 48% HBr in the presence of Aliquat 336 yielded 4c. *n*-Hexylbromide, dm8* bromide and 4c were used to alkylate 5 in DMF at 70°C with K_2CO_3 as base to generate 6a,b,c. Reduction of 6a,b,c with $LiAlH_4$ in THF at 23°C yielded 7a,b,c which

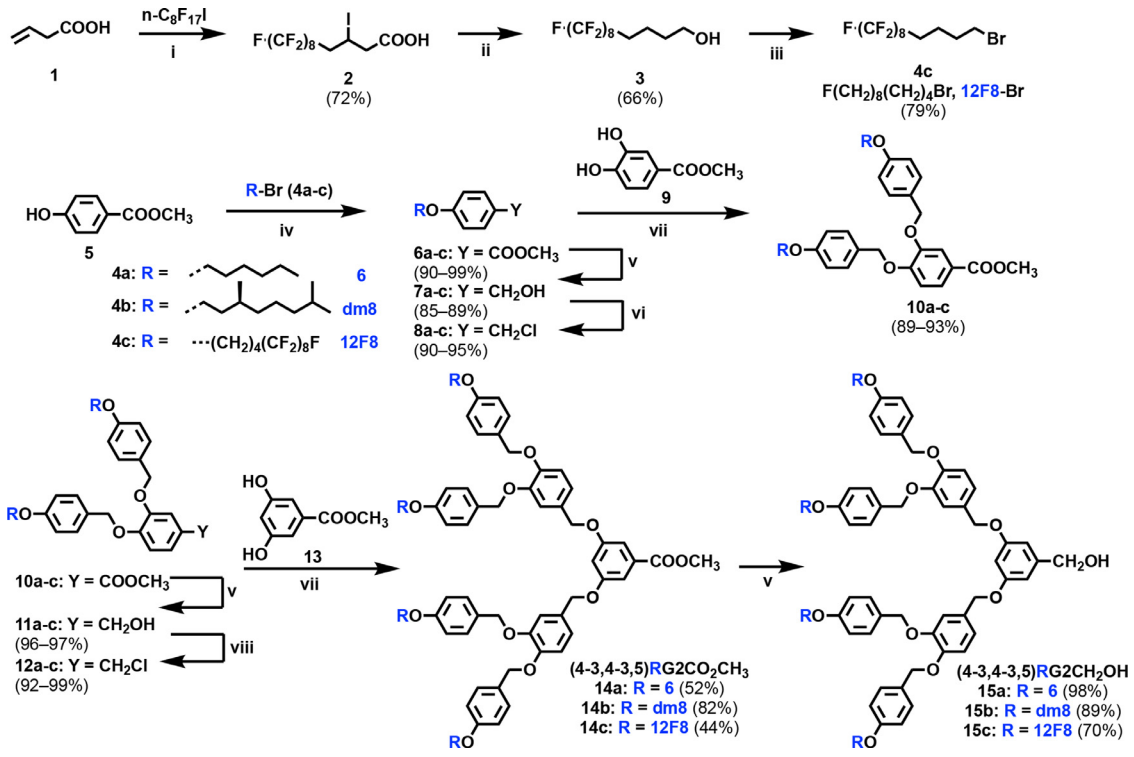

Fig. 1

Synthesis of (4-3,4-3,5)-X, X = $RG_2CO_2CH_3$ or RG_2CH_2OH, R = C_6H_{13}, (*S*)-3,7-dimethyloctyl (dm8*), or $(CH_2)_4(CF_2)_8F$ (12F8). Reagents and conditions: i) $Pd(PPh_3)_4$, hexane, 0–20°C, 10h; ii) $LiAlH_4$, THF, 23°C, 2h; iii) 48% HBr, Aliquat® 336, 100°C, 20h; iv) K_2CO_3, DMF, 70°C, 12h (4a, 4b) or K_2CO_3, DMF, THF, 65°C, 12h (4c); v) $LiAlH_4$, THF, 23°C, 2h; vi) $SOCl_2$, DMF(cat.), DCM, 30 min; vii) K_2CO_3, DMF, 70°C, 12h; viii) $SOCl_2$, DTBMP, DCM, 30 min (12a, 12b) or $SOCl_2$, DCM, C_6H_5-CF_3, 30 min (12c).

after chlorination with $SOCl_2$ with a catalytic amount of DMF in DCM generated 8a,b,c. Alkylation of 9 with 8a,b,c in DMF at 70°C with K_2CO_3 as base yielded 10a,b,c that was reduced with $LiAlH_4$ and subsequently the 11a,b,c were chlorinated with $SOCl_2$ in the presence of a catalytic amount of DMF to form 12a,b,c. Chlorination of 11a,b was performed in DCM while the chlorination of 12c was carried out in C_6H_5-CF_3. In both cases DTBMP was used as a proton trap to avoid the acidic cleavage of the benzyl ether groups. Alkylation of 13 with 12a,b,c produced 14a,b,c which upon reduction with $LiAlH_4$ generated 15a,b,c. Representative MALDI-TOF mass spectra of the semifluorinated dendrons (4-3,4-3,5)12F8G2CO_2CH_3 and (4-3,4-3,5)12F8G2CH_2OH are presented in Fig. 2.

Their DSC traces are shown in Fig. 3 while transition temperatures collected from Fig. 3 together with their enthalpy changes and phases assigned by XRD are summarized in Table 1. Table 2 summarizes the periodic arrays, d-spacings and dimensions of helical supramolecular assembly resulted from the X-ray analysis of oriented fibers of (4-3,4-3,5)-X.

Shockingly, while all supramolecular assemblies exhibit a crystal (Φ_h^k) columnar hexagonal array or a columnar hexagonal array with intracolumnar order (Φ_h^{io}), the compound (4-3,4-3,5)dm8*G2CH_2OH displays also an unexpected A15 Frank-Kasper phase (*Pm*$\bar{3}$*n* space group) [108]. This means that the combination of branched dm8 alkyl tail with the H-bonding at apex induces the transition from tapered to conical dendron that previously could be mediated only by changing the primary structure of the dendron from (4-3,4-3,5)-X to (4-3,4-3,4)-X

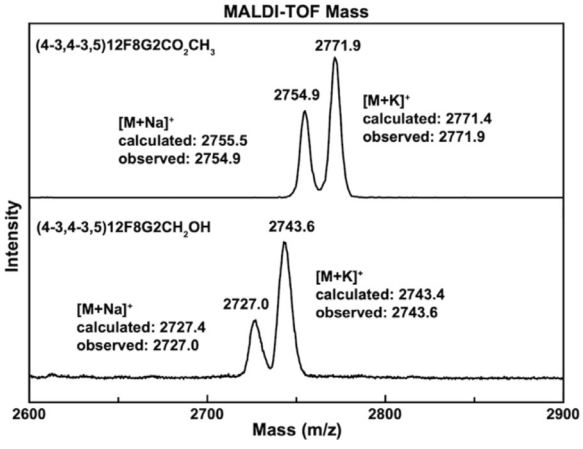

Fig. 2

MALDI-TOF mass spectra of the semifluorinated dendrons (4-3,4-3,5)12F8G2CO_2CH_3 and (4-3,4-3,5)12F8G2CH_2OH.

[62,63,69]. This is a remarkable result since it provides a new mechanism to change the conformation of the self-assembling dendron from tapered to conical shape. No supramolecular orientational memory (SOM) effect was observed on cooling from the A15 to the columnar hexagonal phase and this supports the conical rather than crown conformation of the dendron in the globular supramolecular structure. Fortysix conical dendrons assemble the supramolecular spheres forming this A15 phase (Table 2). However, since a multiple number of transition peaks

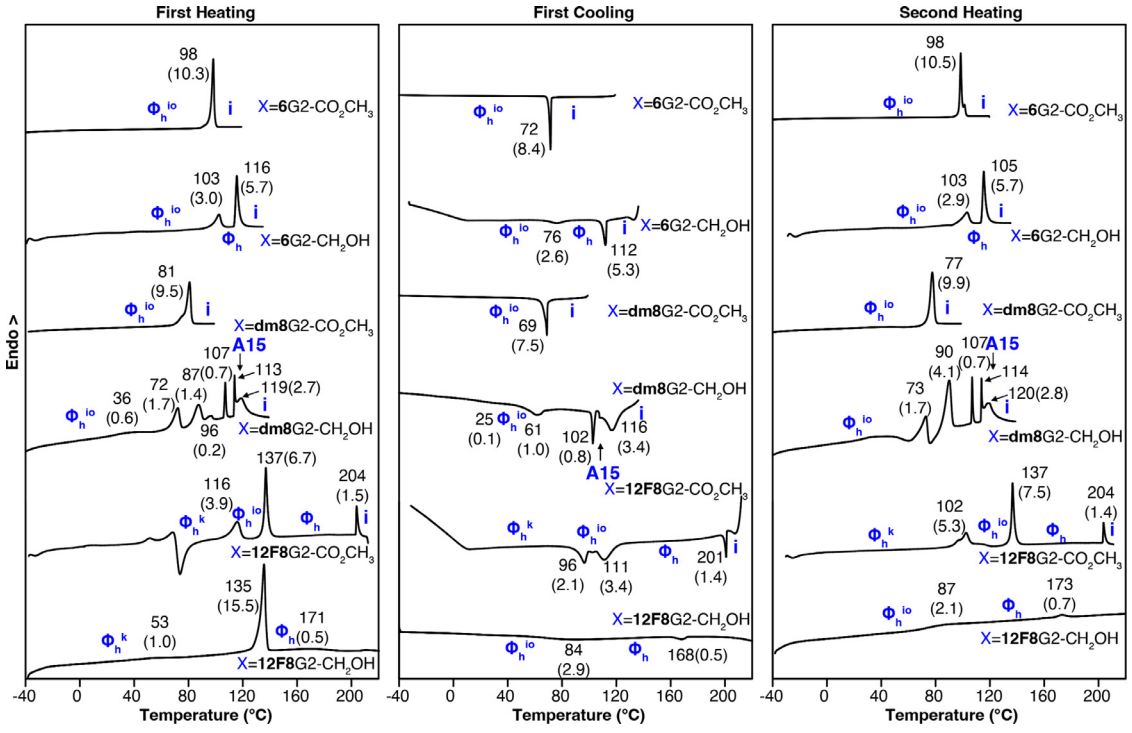

Fig. 3

DSC trances of dendrons (4-3,4-3,5)-X. Phase transition temperatures (°C) and enthalpies (kcal/mol) were indicated. Scanning rate: 10°C/min.

Table 1

Thermal Analysis of the Supramolecular Assemblies of (4-3,4-3,5)-X.

X	Phase transition [°C] and corresponding enthalpy changes (in parenthesis)[kcal mol^{-1}] [a]	
	Heating	**Cooling**
6G2CO_2CH_3	Φ_h^{io} 98 (10.3) i Φ_h^{io} 98 (10.5) i	i 72 (–8.4) Φ_h^{io}
6G2CH_2OH	Φ_h^{io} 103 (3.0) Φ_h 116 (5.7) i Φ_h^{io} 103 (3.0) Φ_h 116 (5.7) i	i 105 (–5.7) Φ_h 103 (–2.9) Φ_h^{io}
dm8*G2CO_2CH_3	Φ_h^{io} 81 (9.5) i Φ_h^{io} 77 (9.9) i	i 69 (–7.5) Φ_h^{io}
dm8*G2CH_2OH	Φ_h^{io} 36 (0.6) Φ_h 72 (1.7) X 84 (1.74) X 96 (0.2), 107 (0.7) A15 113, 119 (2.7) i Φ_h^{io} 73 (1.2) X 90 (4.1) X 107 (0.7) A15 114, 120 (2.8) i	i 116 (–3.4) A15 102 (0.8) Φ_h 61 (1.0) Φ_h^{io}
12F8G2CO_2CH_3	Φ_h^{k} 116 (3.9) Φ_h^{io} 137 (6.7) Φ_h 204 (1.5) i Φ_h^{k} 102 (5.3) Φ_h^{io} 137 (7.5) Φ_h 204 (1.4) i	i 201 (–1.4) Φ_h 111 (–3.4) Φ_h^{io} 96 (2.1) Φ_h^{k}
12F8G2CH_2OH	Φ_h^{k} 53 (1.0) X 135 (15.5) Φ_h 171 (0.5) X Φ_h^{io} 87 (2.1) Φ_h 173 (0.7) X	X 168 (–0.5) Φ_h 84 (–2.9) Φ_h^{io} 8.0

[a] Data from the first heating and cooling scans are on the first line, and data from the second heating are on the second line. Φ_h^{io}: columnar hexagonal lattice with intracolumnar order, Φ_h^{k}: crystalline ordered hexagonal columnar lattice, Φ_h: p6mm hexagonal columnar lattice, i: isotropic, A15: *Pm*$\bar{3}$*n* cubic lattice, X: unknown phase.

are available in a close range of temperature in the DSC of this structure (Fig. 3), X-ray synchrotron experiments performed with variable temperature are needed to provide a complete assignment of all these phase transitions and phases. Due to travel restrictions, they cannot be performed at this time. However, when they will become available, they will be reported in a different publication. A qualitative inspection of Table 2 indicates that all supramolecular columns exhibit diameters that are relatively close in size (44.3 to 52.8 Å) except for the semifluorinated columns that display diameters of 63.5 and 60.1 Å. In all cases the diameters of columns containing H-bonding at the apex is slightly smaller than the corresponding one with ester group at the apex (Table 2).

Table 2

Periodic Arrays, d-Spacings, and Dimensions of Helical Supramolecular Assemblies of (4-3,4-3,5)-X.

X	T (°C)	phase	A (Å)	$d_{10}, d_{11}, d_{20}, d_{21}, d_{30}, d_{22}$ (Å) $d_{110}, d_{200}, d_{210}, d_{211}, d_{220}, d_{310}, d_{222}, d_{320}, d_{321}, d_{400}$ (Å)	D_{column} or D_{sphere} [a] (Å)	ρ (g•cm^3)	μ [b,c]
6G2CO$_2$CH$_3$	30	Φ_h^{io}	49.2	42.6, 24.5, 21.4, 16.1	49.2	1.12	4.2
6G2CH$_2$OH	30	Φ_h^{io}	44.3	38.5, 22.1, 19.1	44.3	1.12	3.5
	110	Φ_h	45.2	39.0, 22.5, 19.5	45.2	1.12	3.6
dm8*G2CO$_2$CH$_3$	30	Φ_h^{io}	52.8	45.7, 26.4, 22.9	52.8	1	3.6
dm8*G2CH$_2$OH	30	Φ_h^{io}	48.6	41.9, 24.2, 21.2	48.6	1	3.2
	110	A15	94.1	66.4, 46.9, 42.2, 38.5, 34.3, 29.8, 27.2, 26.2, 25.2, 23.6	58.4	1	46
12F8G2CO$_2$CH$_3$	130	Φ_h^{io}	63.5	55.1, 32.0, 27.3, 20.7, 18.2, 15.8	63.5	1.5	4.0
12F8G2CH$_2$OH	130	Φ_h^{io}	60.1	51.7, 30.3, 26.0, 19.8, 17.4	60.1	1.5	3.7

[a] for columnar hexagonal phases D_{column}=a, and for the *Pm*$\bar{3}$*n* cubic phases $D_{sphere} = 2\sqrt[3]{3a^3/(32\pi)}$

[b] for columnar hexagonal phases number of dendrons per column strata of thickness $t = 3.5$Å is computed using $\mu = \sqrt{3}a^2 t\rho N_A/(2M_{wt})$ where N_A=Avogadro's number.

[c] for the *Pm*$\bar{3}$*n* cubic phases the average number of dendrons per supramolecular sphere is computed using $\mu = a^3\rho N_A/(8M_{wt})$.

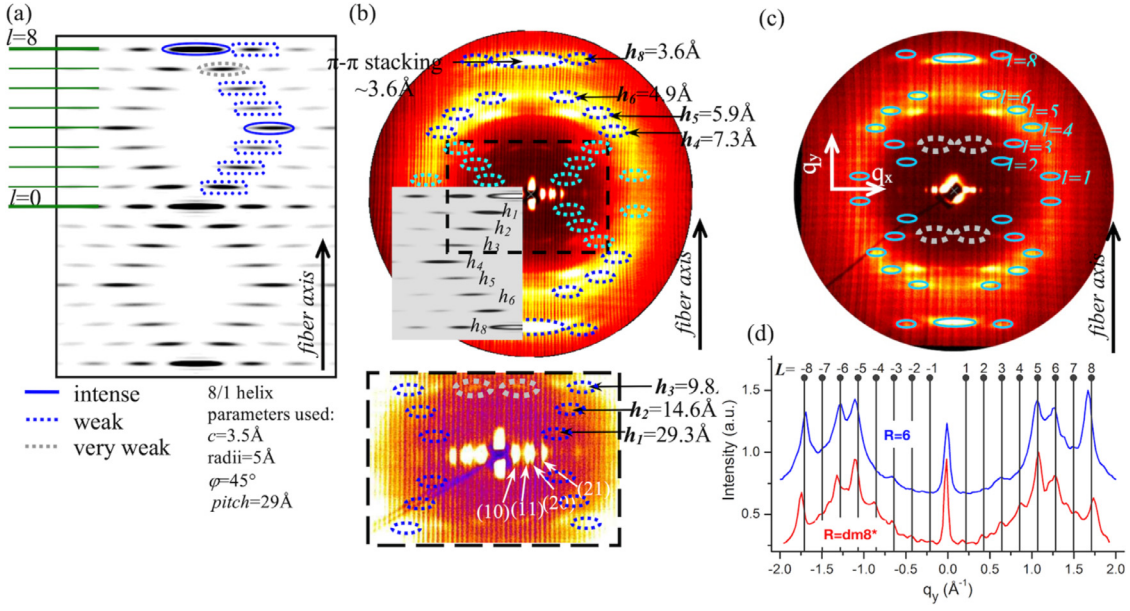

Fig. 4

(4-3,4-3,5)**R**G2CH$_2$OH simulated (a) and measured X-ray diffraction fiber pattern for **R**=**6** (b) and **R**=**dm8*** (c). All the observed helical layer lines fit to an 8/1 helical packing of the dendrons aromatic region, no change of the helical pitch is observed between the achiral or chiral tails structures (d).

The most important feature is that semifluorinated columns contain 5 and respectively 6 d-spacings while the corresponding hydrogenated columns contain 3 or maximum 4 d-spacings (Table 2).

Fig. 4a shows the simulated fiber XRD for the assembly formed from (4-3,4-3,5)6G2CH$_2$OH and the experimental fiber X-ray diffractograms for the same assembly in Fig. 4b and for the assembly of (4-3,4-3,5)dm8*G2CH2OH in Fig. 4c,d. All the observed layer lines fit an 8/1 helical packing of the aromatic region of the dendron in the column. There are only few differences between the simulated and experimental fiber XRD patterns. They are determined by the following features. Experimental XRD corresponds to crystalline structures. The simulated XRD fiber patterns rely on single column simulation since the space group of the crystal is unknown. In other words, simulation does not account for 3-dimensional intercolumnar correlations which may explain the absence of features on L=7 and the additional features observed on L=5. No change in the helical pitch is observed between the achiral and chiral tails structures (Fig. 4d). The calculation of the helix radius from the q_x vs intensity plots of the fiber pattern of the assembly generated from (4-3,4-3,5)dm8*G2CH2OH of Fig. 1c is shown in Fig. 5.

The positions of the corresponding layer line maxima are marked with red arrows. A schematic representation of the helix parameters of the 8/1 helix and of the ideal fiber diffraction patterns are illustrated in Fig. 6. Fig. 6a shows the 8/1 helix based on one high electron density region located at 5 Å radii from the column axis while Fig. 6b shows the 8/1 helix based on two

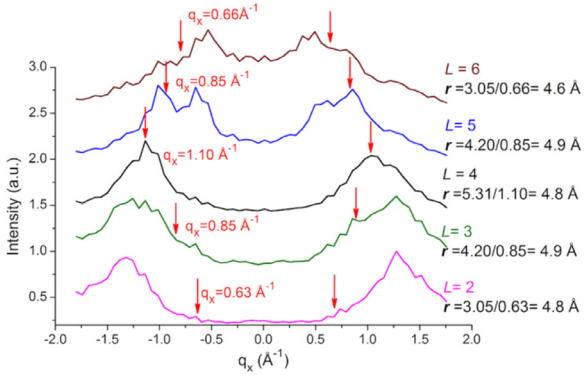

Fig. 5

Helix radius calculation from the q_x vs intensity plots of the (4-3,4-3,5)**dm8***-G2CH$_2$OH fiber pattern from Fig. 4c. The positions of the corresponding layer line maxima are marked by the red arrows.

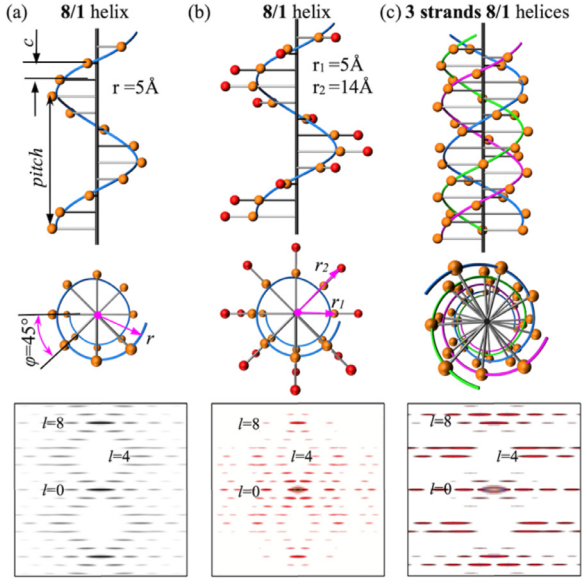

Fig. 6

Schematic of the 8/1 helix, helix parameters and ideal diffraction fiber patterns: (a) 8/1 helix based on one high electron density region located at 5Å radii from column axis; (b) 8/1 helix based on two high electron density regions located at 5Å and respectively 14Å radii from column axis; (c) three interlocked 8/1 helical strands. In (a), (b), (c): top- side view of the helix, middle- top view of the helix, and bottom- the corresponding simulated diffraction fiber pattern.

high electron density regions located at 5 Å and respectively at 14 Å radii from the column axis. Three interlocked 8/1 helical strands are shown in Fig. 6c. In all cases, a,b,c the side view of the helix is shown on top, the top view is shown in the middle while the corresponding simulated diffraction patterns are shown in the bottom.

Fig. 7 shows the simulation of the fiber diffraction by Cerius^2 based on the reconstructed molecular model of the helical column assemble from (4-3,4-3,5)RG2CH$_2$OH. Only the aromatic core region of the helical column was used in this simulation in order to limit the broadening that would be generated by the incorporation of the alkyl chains in the column structure. This molecular model will be discussed later.

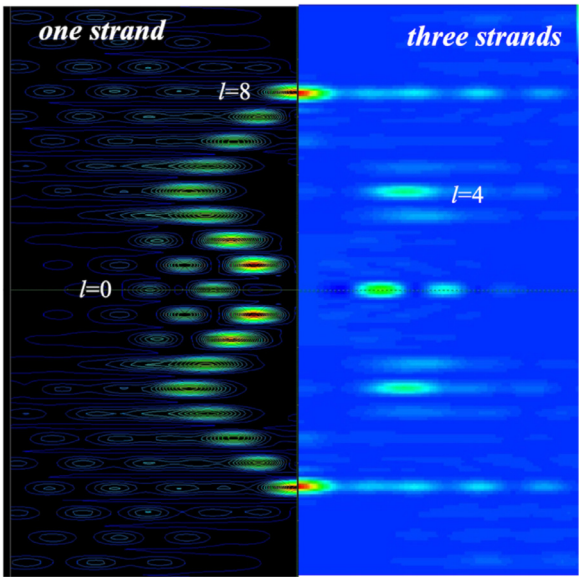

Fig. 7

Fiber diffraction Cerius^2 simulation based on the reconstructed molecular model of the (4-3,4-3,5)**R**G2CH$_2$OH. Only the aromatic core region was used in the simulation to limit the broadening caused by the inclusion of the alkyl chains.

The experimental fiber diffractograms of all structures are combined in Fig. 8a and their meridional q-plots are shown in Fig. 8b. Only a very small variation of the π-π stacking correlation feature labeled at L=8 as a function of dendron peripheral substitution hydrogenated achiral vs chiral and vs semifluorinated was observed in Fig. 8b. However, no change in L=8 is observed at the transition from alcohol to ester at the apex (Fig. 8). The difference between the order in the helix is best seen from the combination of Fig. 8a with vertical fiber axis and Fig. 8, as qualitatively was shown in Table 2.

The highest number of diffractions was observed in semifluorinated columns with the H-bonded apex perfluorinated columns showing the highest order. Small angle diffraction plots of all assemblies at different temperatures, indexing of diffraction peaks and the diameters of the columns are shown in Fig. 9 and 10. Fig. 9a shows the wide-angle X-ray diffraction oriented fiber patters collected at 30°C together with an overlaid 8/1 helix simulation of the helical column assemble from (4-3,4-3,5)12F8G2CO$_2$CH$_3$. The fiber pattern simulation of and 8/1 helix with two objects positioned at the radii of 6 Å and respectively 20 Å of the same structure are shown in Fig. 9b. This simulation explains the appearance of lower q-values on the L=3 layer line. This feature is indicated by the gray dotted circle in both Fig. 9a and 9b. Fig. 9c shows the wide-angle oriented fiber diffractogram of the same assembly at 130°C in the upper half and at 160°C in the bottom half. These diffractograms indicate a gradual diffusion of the fluorinated region boundary with the increase of the temperature. The small angle of the same column at 30°C in the upper half and 160°C in the lower half of the diffractograms demonstrating the fiber alignment and the change in (hk0) reflection intensities and the lattice parameter as a function of temperature. As expected, there is a small decrease

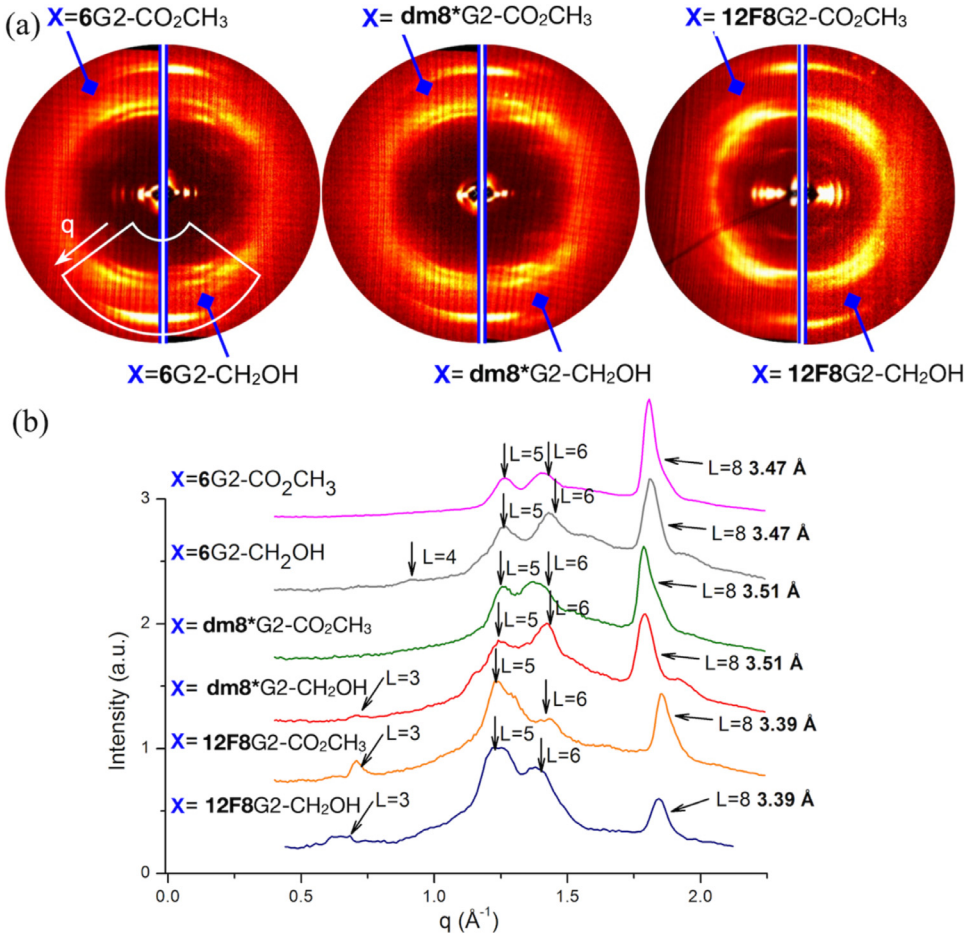

Fig. 8

(4-3,4-3,5)-**X** wide angle diffraction fiber pattern collected at 24°C (a) and their corresponding meridional q-plots (b). Slight variation of the π-π stacking correlation feature (labeled as L=8) as a function of dendron peripheral substitution (chiral or achiral hydrogenated or semi-fluorinated tails) and no change as a function of the dendron apex functional group (alcohol or ester). In (a) the fiber axis is vertical.

of the lattice parameter a from 62.7 Å to 61.1 Å as the temperature increases from 30°C to 160°C due to small compression of the column. Most of the XRD patterns parameters are already listed in Figs. 4d, 5 and 8b. Once higher resolution data from synchrotron experiments will become available we will attempt assignment of space groups for the columnar hexagonal crystal phases which will allow to make distinction between 3-D column-to-column correlations and intramolecular helical features.

The comparison of the 3-level fit of the experimentally measured shown in squares and of the fitted shown in circles amplitudes of the wide-angle X-ray diffraction plot and pattern for the (4-3,4-3,5)12F8G2CO_2CH_3 supramolecular columns at 100°C are shown in Fig. 11a,b. The lines are indicating the expected peak position of the columnar hexagonal lattices calculated using the lattice parameter a = 62.6 Å. The same excellent agreement was observed between the powder X-ray plots at 130°C and 160°C (Fig. 12a,b) and the measured, in squares, and 3-level fit calculated, shown in circles, for the helical supramolecular columns of (4-3,4-3,5)12F8G2CH_2OH (Fig. 12c). The 3-level fit agreement between experimental and modeled XRD intensities, used to determine the pore size diameters reported in Fig. 10, is shown in Fig. 11b for (4-3,4-3,5)**12F8**G2CO_2CH_3 and Fig. 12c for (4-3,4-3,5)**12F8**G2CH_2OH.

The accuracy of the data from Fig. 11 and 12 allowed the determination of the 2-D and 3D electron density maps for the supramolecular perfluorinated columns of (4-3,4-3,5)12F8G2CH_2OH (Fig. 13) and of (4-3,4-3,5)12F8G2CO_2CH_3 (Fig. 14). The solutions for the electron density maps that will be shown and discussed in Figs. 13 and 14 were selected based on matching electron density computed from molecular models as well as from 3-level fit solutions reported in Figs. 11b and 12c.

The 2-D and 3-D surfaces of the reconstructed relative electron density maps obtained for the columns of (4-3,4-3,5)12F8G2CH_2OH at 130°C are shown in Fig. 13a and b while the same data for the 160°C are shown in Fig. 13c,d. The diffusion of the fluorinated-hydrogenated boundary observed in the compound with the ester at the apex in Fig. 9 is observed also here. In the red colored region these significant changes are indicated by the double arrows from a,b,c,d parts of Fig. 13. The second important conclusion of these experiments is that these columns are porous similar to those assembled from dendritic dipeptides [62] except that their synthetic design is much simpler.

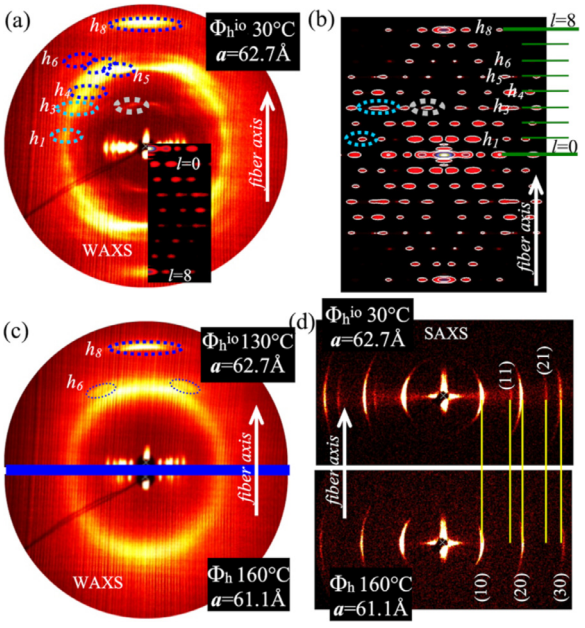

Fig. 9

(4-3,4-3,5)**12F8**G2CO$_2$CH$_3$ wide angle X-ray fiber diffraction: fiber pattern collected at 30°C together with the overlaid 8/1 helix simulation (a); the fiber pattern simulation of a 8/1 helix with two objects positioned at the radii of 6Å and respectively 20Å explain the appearance at lower *q*-values on the *l*=3 layer line (features indicated by the gray dotted circles in a and b) (b); fiber pattern collected at 130°C (upper half) and 160°C (lower half) indicating a gradual diffusion of the fluorinated region boundary with the increasing of temperature (c); corresponding small angle fiber pattern collected at the indicated temperatures showing the fiber alignment and changes in the relative (hk0) reflection intensities (d).

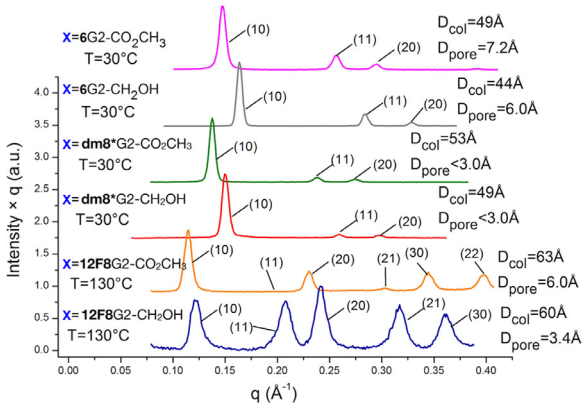

Fig. 10

Small angle powder diffraction plots for the assemblies of (4-3,4-3,5)-**X**. X, temperature, lattice parameters and peaks are indicated.

The pore diameter D_{pore}=3.4±1.56 Å at 130°C and 3.6±1.7 Å at 160°C. A similar conclusion with slightly larger pore diameters were demonstrated by the electron density maps shown in Fig. 14.

The detailed molecular model of the helical supramolecular column assembled from (4-3,4-3,5)dm8*G2CH$_2$OH is shown in Fig. 15 while the wide angle X-ray q_y-plots of the fiber patterns of all helical structures are shown in Fig. 16.

Conclusions

One of the best investigated helical columnar forming dendron was equipped with different functional groups at its apex and of its alkyl group periphery and its self-assembly was investigated with a combination of DSC, powder, small-angle and wide-angle oriented fiber X-ray diffraction methodologies, helical diffraction theory and 2-D and 3-D reconstructed electron density maps. Principles responsible for the creation of high helical order were elaborated. These principles will be used to program order and functions in supramolecular assemblies and bring the interest of

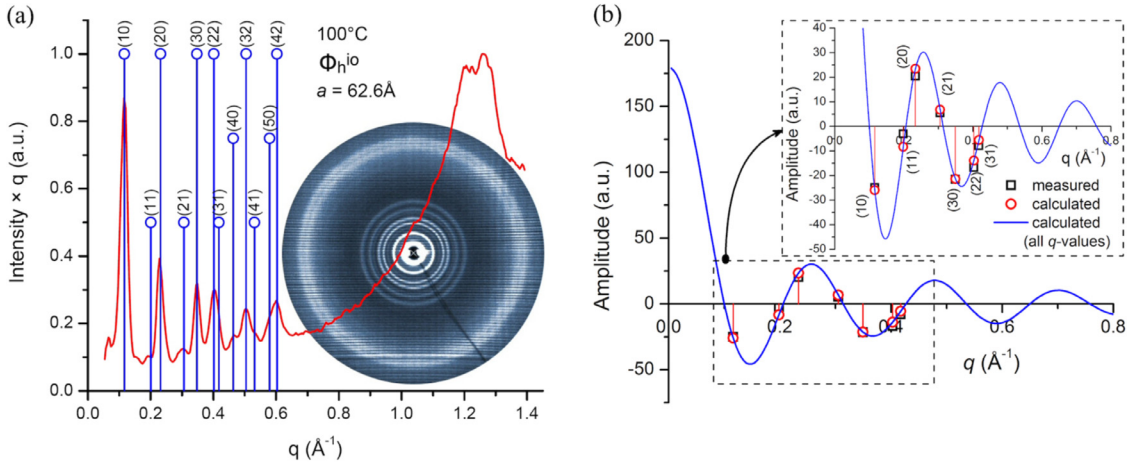

Fig. 11

Wide angle X-ray diffraction plot and pattern of the perfluorinated columns assembled from (4-3,4-3,5)**12F8**G2CO$_2$CH$_3$ (a) and 3-level fit comparison of the measured (squares) and fitted (circles) amplitudes for the 100°C data (b). The lines are indicating the expected peak position of the columnar hexagonal lattices calculated using the lattice parameter a = 62.6 Å.

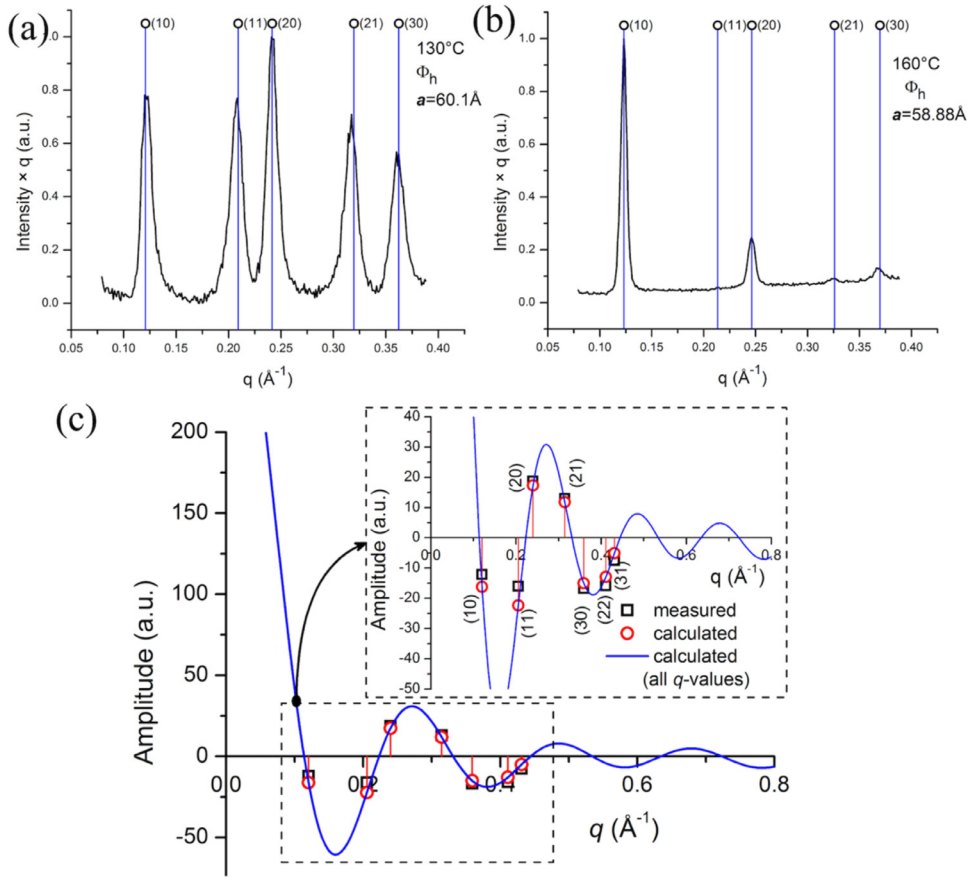

Fig. 12

Powder X-ray plots at 130°C for the assemblies of (4-3,4-3,5)**12F8**G2CH$_2$OH (a) and 160°C (b). Agreement between the measured (squares) and 3-level fit calculated (circles) powder diffraction amplitudes (c).

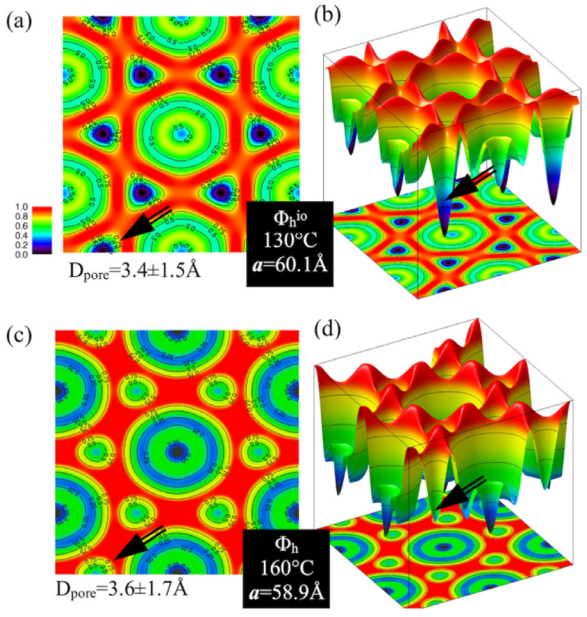

Fig. 13

(4-3,4-3,5)**12F8**G2CH_2OH 2-dimensional assemblies (a, c) and 3-dimensional surface (b, d) reconstructed relative electron densities. The same diffusion of the fluorinated-hydrogenated boundary from the ester (Fig. 10) is observed (in the red colored region the significant changes are indicated by the double arrows).

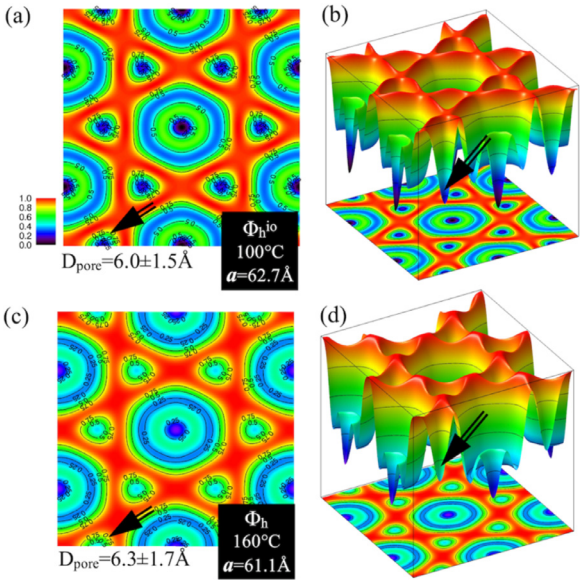

Fig. 14

(4-3,4-3,5)**12F8**G2CO_2CH_3 2-dimensional (a, b) and 3-dimensional surface (c, d) reconstructed relative electron densities. As the powder and fiber data (Fig. 10) indicates, the maps confirm a diffusion of the fluorinated-hydrogenated boundary as the electron density distribution in the aliphatic region is indicating (in the red colored region the significant changes are indicated by the double arrows).

additional research groups to determine the structure of their supramolecular assemblies by X-ray diffraction methodologies elaborated here and in other related publications [39–44, 211–231]. Linear, branched and semifluorinated alkyl groups were used on the periphery together with H-bonding and non-H-bonding groups at the apex. Unexpectedly a combination of branched alkyl groups on the periphery together with H-bonding at the apex of the dendron generated a new mechanism for the transition

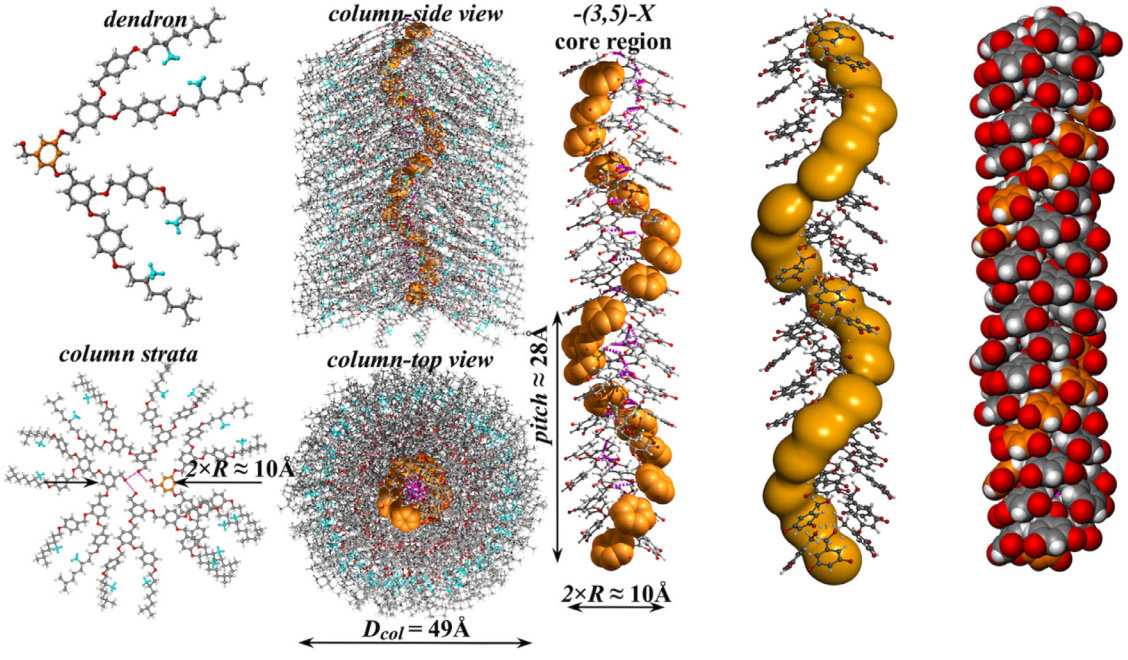

Fig. 15

X=**dm8***CH_2OH molecular model. Color code: chiral methyl (s)-CH_3- blue; C- gray; H- white; O- red; one of the (3,5) aromatic ring- gold; H-bonding network- magenta.

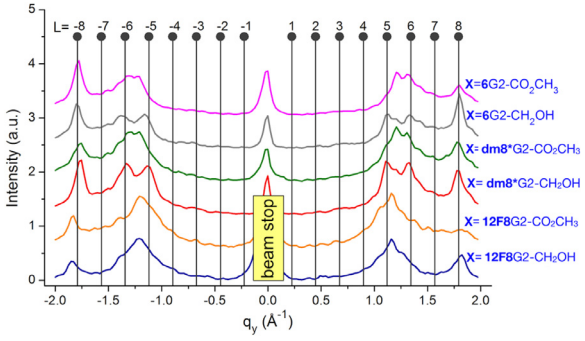

Fig. 16

Wide angle XRD q_y-plots of the fiber patterns shown in Fig. 10. L= layer line.

from tapered to conical dendron that mediated the transition from a columnar hexagonal array to an A15 Frank-Kasper phase generated from supramolecular spheres. Semifluorination of the dendron provided together with both non-H-bonding and H-bonding functional groups at the apex the simplest perfluorinated porous helical columns of interest for water transport and purification. The detailed contribution of each functional group to the creation of order was discussed. H-bonding at the apex together with semifluorination on the periphery provided the higher helical order of the columns. These structure-order principles can be exploited to program high order functional systems with numerous applications.

Declaration of Competing Interest

The authors declare no competing interests in this paper.

Acknowledgement

Financial support by the National Science Foundation (DMR-1807127, DMR-1720530, and DMR- 2104554), the Humboldt Foundation, and the P. Roy Vagelos Chair at Penn (all to V.P.) is gratefully acknowledged.

References

[1] S. Chandrasekhar, B.K. Sadashiva, K.A. Suresh, Liquid crystals of disc-like molecules, Pramana - J Phys 9 (1977) 471–480, doi:10.1007/BF02846252.

[2] T. Wöhrle, I. Wurzbach, J. Kirres, A. Kostidou, N. Kapernaum, J. Litterscheidt, J.C. Haenle, P. Staffeld, A. Baro, F. Giesselmann, S. Laschat, Discotic liquid crystals, Chem. Rev. 116 (2016) 1139–1241, doi:10.1021/acs.chemrev.5b00190.

[3] S. Laschat, A. Baro, N. Steinke, F. Giesselmann, C. Hägele, G. Scalia, R. Judele, E. Kapatsina, S. Sauer, A. Schreivogel, M. Tosoni, Discotic liquid crystals: from tailor-made synthesis to plastic electronics, Angew. Chem. Int. Ed. 46 (2007) 4832–4887, doi:10.1002/anie.200604203.

[4] W. Kranig, H.W. Spiess, H. Zimmermann, Substituted tetrabenzocyclophanes as mesogenic units of new polycondensates exhibiting columnar mesophases, Liq. Cryst. 7 (1990) 123–129, doi:10.1080/02678299008029199.

[5] H. Zimmermann, Tetrabenzocyclododecatetraene A new core for mesogens exhibiting columnar mesophases, Liq. Cryst. 3 (1988) 759–770, doi:10.1080/02678298808086532.

[6] V. Percec, C.G. Cho, C. Pugh, D. Tomazos, Synthesis and characterization of branched liquid-crystalline polyethers containing cyclotetraveratrylene-based disk-like mesogens, Macromolecules 25 (1992) 1164–1176, doi:10.1021/ma00029a025.

[7] V. Percec, C.G. Cho, C. Pugh, Cyclotrimerization versus cyclotetramerization in the electrophilic oligomerization of 3,4-bis(methyloxy)benzyl derivatives, Macromolecules 24 (1991) 3227–3234, doi:10.1021/ma00011a029.

[8] V. Percec, C.G. Cho, C. Pugh, Alkyloxy-substituted CTTV derivatives that exhibit columnar mesophases, J. Mater. Chem. 1 (1991) 217–222, doi:10.1039/JM9910100217.

[9] J. Malthete, A. Collet, Inversion of the cyclotribenzylene cone in a columnar mesophase: a potential way to ferroelectric materials, J. Am. Chem. Soc. 109 (1987) 7544–7545, doi:10.1021/ja00258a057.

[10] J. Malthete, A. Collet, A.-M. Levelut, Mesogens containing the DOBOB group, Liq. Cryst. 5 (1989) 123–131, doi:10.1080/02678298908026355.

[11] V. Percec, M.R. Imam, M. Peterca, D.A. Wilson, P.A. Heiney, Self-assembly of dendritic crowns into chiral supramolecular spheres, J. Am. Chem. Soc. 131 (2009) 1294–1304, doi:10.1021/ja8087778.

[12] V. Percec, M.R. Imam, M. Peterca, D.A. Wilson, R. Graf, H.W. Spiess, V.S.K. Balagurusamy, P.A. Heiney, Self-assembly of dendronized triphenylenes into helical pyramidal columns and chiral spheres, J. Am. Chem. Soc. 131 (2009) 7662–7677, doi:10.1021/ja8094944.

[13] H.-T. Nguyen, C. Destrade, J. Malthécte, Phasmids and polycatenar mesogens, Adv. Mater. 9 (1997) 375–388, doi:10.1002/adma.19970090503.

[14] J.A. Heck, Supramolecular polymers, Master of Science thesis, Case Western Reserve University, 1992.

[15] V. Percec, J. Heck, Abstr. Pap. Am. Chem. Soc. 198 (1989) 135 –Poly.

[16] V. Perec, J. Heck, Side-chain liquid-crystal polymers containing mesogenic units based on 1/2 disk and rod-like moieties, ACS Polym. Prepr. 30 (1989) 450.

[17] V. Percec, J. Heck, Liquid crystalline polymers containing mesogenic units based on half-disc and rod-like moieties, Polym. Bull. 24 (1990) 255–262, doi:10.1007/BF00306572.

[18] V. Percec, J. Heck, Liquid-crystalline polymers containing mesogenic units based on half-disk and rod-like moieties. 3. Synthesis and characterization of polymethylsiloxanes and copolymethyl-siloxanes based on 4-[3,4,5-tri(p-N-dodecan-1-yloxybenzyloxy)benzoate]-4′-(p-allyloxybenzoate)biphenyl and 4-[3,4,5-tri(p-N-dodecan-1-yloxy-benzyloxy)benzoate]-4′-(p-allyloxybenzo ate)thiodiphenyl side groups, Polym. Bull. 25 (1991) 55–62, doi:10.1007/BF00338899.

[19] V. Percec, J. Heck, Liquid crystalline polymers containing mesogenic units based on half-disc and rod-like moieties, Polym. Bull. 25 (1991) 431–438, doi:10.1007/BF00310233.

[20] V. Percec, J. Heck, Liquid crystalline polymers containing mesogenic units based on half-disc and rod-like moieties. I. Synthesis and characterization of 4-(11-undecan-1-yloxy)-4′-[3,4,5-tri(p-n-dodecan-1-yloxybenzyloxy)benzoate]biphenyl side groups, J. Polym. Sci. Part A: Polym. Chem. 29 (1991) 591–597, doi:10.1002/pola.1991.080290416.

[21] V. Percec, J. Heck, G. Ungar, Liquid-crystalline polymers containing mesogenic units based on half-disk and rodlike moieties. 5. Side-chain liquid-crystalline poly(methylsiloxanes) containing hemiphasmidic mesogens based on 4-[[3,4,5,-tris(alkan-1-yloxy)benzoyl]oxy]-4′-[[p-(propan-1-yloxy)benzoyl]oxy]biphenyl groups, Macromolecules 24 (1991) 4957–4962, doi:10.1021/ma00017a036.

[22] J.A. Heck, PhD Thesis, Case Western Reserve University, 1995.

[23] V. Percec, J. Heck, M. Lee, G. Ungar, A. Alvarez-Castillo, Poly{2-vinyloxyethyl 3,4,5-tris[4-(n-dodecanyloxy)benzyloxy]benzoate}: a self-assembled supramolecular polymer similar to tobacco mosaic virus, J. Mater. Chem. 2 (1992) 1033–1039, doi:10.1039/JM9920201033.

[24] V. Percec, M. Lee, J. Heck, H.E. Blackwell, G. Ungar, A. Alvarez-Castillo, Re-entrant isotropic phase in a supramolecular disc-like oligomer of 4-[3,4,5-tris(n-dodecanyloxy)benzoyloxy]-4′-[(2-vinyloxy)ethoxy]biphenyl, J. Mater. Chem. 2 (1992) 931–938, doi:10.1039/JM9920200931.

[25] V. Percec, G. Johansson, J. Heck, G. Ungarb, S.V. Battyb, Molecular recognition directed self-assembly of supramolecular cylindrical channel-like architectures from 6,7,9,10,12,13,15,16-octahydro-1,4,7,10,13-pentaoxabenzocyclopentadecen-2-ylmethyl 3,4,5-tris(p-dodecyloxybenzyloxy)benzoate, J. Chem. Soc., Perkin Trans. 1 (1993) 1411–1420, doi:10.1039/P19930001411.

[26] V. Percec, J. Heck, D. Tomazos, F. Falkenberg, H. Blackwell, G. Ungar, Self-assembly of taper-shaped monoesters of oligo(ethylene oxide) with 3,4,5-tris(p-dodecyloxybenzyloxy)benzoic acid and of their polymethacrylates into tubular supramolecular architectures displaying a columnar mesophase, J. Chem. Soc., Perkin Trans. 1 (1993) 2799–2811, doi:10.1039/P19930002799.

[27] V. Percec, J.A. Heck, D. Tomazos, G. Ungar, The influence of the complexation of sodium and lithium triflate on the self-assembly of tubular-supramolecular architectures displaying a columnar mesophase based on taper-shaped monoesters of oligoethylene oxide with 3,4,5-tris[p-(n-dodecan-1-yloxy)benzyloxy]benzoic acid and of their polymethacrylates, J. Chem. Soc., Perkin Trans. 2 (1993) 2381–2388, doi:10.1039/P29930002381.

[28] G. Johansson, V. Percec, G. Ungar, D. Abramic, Molecular recognition directed self-assembly of tubular liquid crystalline and crystalline supramolecular architectures from taper shaped (15-crown-5)methyl 3,4,5-tris(p-alkyloxybenzyloxy)benzoates and (15-crown-5)methyl 3,4,5-tris(p-dodecyloxy)benzoate, J. Chem. Soc., Perkin Trans. 1 (1994) 447–459, doi:10.1039/P19940000447.

[29] V. Percec, D. Tomazos, J. Heck, H. Blackwell, G. Ungar, Self-assembly of taper-shaped monoesters of oligo(ethylene oxide) with 3,4,5-tris(n-dodecan-1-yloxy)benzoic acid and of their polymethacrylates into tubular supramolecular architectures displaying a columnar hexagonal mesophase, J. Chem. Soc., Perkin Trans. 2 (1994) 31–44, doi:10.1039/P29940000031.

[30] V. Percec, D. Schlueter, G. Ungar, S.Z.D. Cheng, A. Zhang, Hierarchical control of internal superstructure, diameter, and stability of supramolecular and macromolecular columns generated from tapered monodendritic building blocks, Macromolecules 31 (1998) 1745–1762, doi:10.1021/ma971459p.

[31] Y.K. Kwon, S. Chvalun, A.-I. Schneider, J. Blackwell, V. Percec, J.A. Heck, Supramolecular tubular structures of a polymethacrylate with tapered side groups in aligned hexagonal phases, Macromolecules 27 (1994) 6129–6132, doi:10.1021/ma00099a029.

[32] Y.K. Kwon, S.N. Chvalun, J. Blackwell, V. Percec, J.A. Heck, Effect of temperature on the supramolecular tubular structure in oriented fibers of a poly(methacrylate) with tapered side groups, Macromolecules 28 (1995) 1552–1558, doi:10.1021/ma00109a029.

[33] V. Percec, D. Schlueter, Y.K. Kwon, J. Blackwell, M. Moeller, P.J. Slangen, Dramatic stabilization of a hexagonal columnar mesophase generated from supramolecular and macromolecular columns by the semifluorination of the alkyl groups of their tapered building blocks, Macromolecules 28 (1995) 8807–8818, doi:10.1021/ma00130a013.

[34] V. Percec, D. Schlueter, J.C. Ronda, G. Johansson, G. Ungar, J.P. Zhou, Tubular architectures from polymers with tapered side groups. Assembly of side groups via a rigid helical chain conformation and flexible helical chain conformation induced via assembly of side groups, Macromolecules 29 (1996) 1464–1472, doi:10.1021/ma951244k.

[35] V. Percec, D. Schlueter, Mechanistic investigations on the formation of supramolecular cylindrical shaped oligomers and polymers by living ring opening metathesis polymerization of a 7-oxanorbornene monomer substituted with two tapered monodendrons, Macromolecules 30 (1997) 5783–5790, doi:10.1021/ma970157k.

[36] V. Percec, J. Heck, G. Johansson, D. Tomazos, M. Kawasumi, G. Ungar, Molecular-recognition-directed self-assembly of supramolecular polymers, J. Macromol. Sci, Part A. Pure Appl. Chem. 31 (1994) 1031–1070, doi:10.1080/10601329409349776.

[37] V. Percec, Bioinspired supramolecular liquid crystals, Phil. Trans. R. Soc. A 364 (2006) 2709–2719, doi:10.1098/rsta.2006.1848.

[38] V. Percec, Q. Xiao, The legacy of Rosalind E. Franklin: Landmark contributions to two Nobel Prizes, Chem 7 (2021) 529–536, doi:10.1016/j.chempr.2021.02.020.

[39] V. Percec, Merging macromolecular and supramolecular chemistry into bioinspired synthesis of complex systems, Isr. J. Chem. 60 (2020) 48–66, doi:10.1002/ijch.202000004.

[40] V. Percec, Q. Xiao, Helical self-organizations and emerging functions in architectures, biological and synthetic macromolecules, Bull. Chem. Soc. Jpn. 94 (2021) 900–928, doi:10.1246/bcsj.20210015.

[41] C. Roche, V. Percec, Complex adaptable systems based on self-assembling dendrimers and dendrons: Toward dynamic materials, Isr. J. Chem. 53 (2013) 30–44, doi:10.1002/ijch.201200099.

[42] V. Percec, Q. Xiao, Helical chirality of supramolecular columns and spheres self-organizes complex liquid crystals, crystals, and quasicrystals, Isr. J. Chem. 61 (2021) 530–565, doi:10.1002/ijch.202100057.

[43] B.M. Rosen, C.J. Wilson, D.A. Wilson, M. Peterca, M.R. Imam, V. Percec, Dendron-mediated self-assembly, disassembly, and self-organization of complex systems, Chem. Rev. 109 (2009) 6275–6540, doi:10.1021/cr900157q.

[44] H.-J. Sun, S. Zhang, V. Percec, From structure to function *via* complex supramolecular dendrimer systems, Chem. Soc. Rev. 44 (2015) 3900–3923, doi:10.1039/C4CS00249K.

[45] V. Percec, Q. Xiao, G. Lligadas, M.J. Monteiro, Perfecting self-organization of covalent and supramolecular mega macromolecules via sequence-defined and monodisperse components, Polymer 211 (2020) 123252, doi:10.1016/j.polymer.2020.123252.

[46] J.G. Rudick, V. Percec, Induced helical backbone conformations of self-organizable dendronized polymers, Acc. Chem. Res. 41 (2008) 1641–1652, doi:10.1021/ar800086w.

[47] J.G. Rudick, V. Percec, Helical chirality in dendronized polyarylacetylenes, New J. Chem. 31 (2007) 1083–1096, doi:10.1039/B616449H.

[48] G. Ungar, J.L. Feijoo, V. Percec, R. Yourd, Liquid-crystalline polyethers based on conformational isomerism. 16. Hexagonal columnar phase (.PHI.h) in a nondiscotic copolyether based on 1,2-bis(4-hydroxyphenyl)ethane, 1,8-dibromooctane, and 1,12-dibromododecane, and the novel 2-dimensional-3-dimensional. PHI.h-sB transition, Macromolecules 24 (1991) 953–957, doi:10.1021/ma00004a023.

[49] V. Percec, M. Zuber, G. Ungar, A. Alvarez-Castillo, Molecular engineering of a hexagonal columnar (.PHI.h) mesophase exhibited by flexible copolyethers based on 1-(4-hydroxyphenyl)-2-(2-R-4-hydroxyphenyl)ethane with R = H, F, and flexible spacers, Macromolecules 25 (1992) 1193–1197, doi:10.1021/ma00029a029.

[50] V. Percec, M. Zuber, S.Z.D. Cheng, A.-Q. Zhang, Liquid-crystalline polyethers based on conformational isomerism. Part 22—Hexagonal columnar mesophase in polyethers and copolyethers based on 1,4-bis[2-(4-hydroxyphenyl)ethyl]benzene, 1,2-bis(4-hydroxyphenyl)ethane and 1,9-dibromononane, J. Mater. Chem. 2 (1992) 407–414, doi:10.1039/JM9920200407.

[51] G. Ungar, J. Zhou, V. Percec, P. Chu, Nematic, smectic and columnar phases of main-chain liquid crystal polyethers, Macromol. Symp. 98 (1995) 951–966, doi:10.1002/masy.19950980183.

[52] V. Percec, D. Schlueter, G. Ungar, Rational design of a hexagonal columnar mesophase in telechelic alternating multicomponent semifluorinated polyethylene oligomers, Macromolecules 30 (1997) 645–648, doi:10.1021/ma961285w.

[53] G. Ungar, Thermotropic hexagonal phases in polymers: common features and classification, Polymer 34 (1993) 2050–2059, doi:10.1016/0032-3861(93)90730-X.

[54] G.H.F. Bergmann, H. Finkelmann, V. Percec, M. Zhao, Liquid-crystalline main-chain elastomers, Macromol. Rapid Commun. 18 (1997) 353–360, doi:10.1002/marc.1997.030180501.

[55] V. Percec, G. Ungar, M. Peterca, Self-assembly in action, Science 313 (2006) 55–56, doi:10.1126/science.1129512.

[56] Y. Li, S.-T. Lin, W.A. Goddard, Efficiency of various lattices from hard ball to soft ball: theoretical study of thermodynamic properties of dendrimer liquid crystal from atomistic simulation, J. Am. Chem. Soc. 126 (2004) 1872–1885, doi:10.1021/ja038617e.

[57] P. Ziherl, R.D. Kamien, Maximizing entropy by minimizing area: Towards a new principle of self-organization, J. Phys. Chem. B. 105 (2001) 10147–10158, doi:10.1021/jp010944q.

[58] C.R. Iacovella, A.S. Keys, S.C. Glotzer, Self-assembly of soft-matter quasicrystals and their approximants, Proc. Natl. Acad. Sci. U.S.A. 108 (2011) 20935–20940, doi:10.1073/pnas.1019763108.

[59] M. Peterca, V. Percec, Recasting metal alloy phases with block copolymers, Science 330 (2010) 333–334, doi:10.1126/science.1196698.

[60] V. Percec, M. Glodde, T.K. Bera, Y. Miura, I. Shiyanovskaya, K.D. Singer, V.S.K. Balagurusamy, P.A. Heiney, I. Schnell, A. Rapp, H.-W. Spiess, S.D. Hudson, H. Duan, Self-organization of supramolecular helical dendrimers into complex electronic materials, Nature 419 (2002) 384–387, doi:10.1038/nature01072.

[61] V. Percec, A.E. Dulcey, M. Peterca, M. Ilies, M.J. Sienkowska, P.A. Heiney, Programming the internal structure and stability of helical pores self-assembled from dendritic dipeptides via the protective groups of the peptide, J. Am. Chem. Soc. 127 (2005) 17902–17909, doi:10.1021/ja056313h.

[62] V. Percec, A.E. Dulcey, V.S.K. Balagurusamy, Y. Miura, J. Smidrkal, M. Peterca, S. Nummelin, U. Edlund, S.D. Hudson, P.A. Heiney, H. Duan, S.N. Magonov, S.A. Vinogradov, Self-assembly of amphiphilic dendritic dipeptides into helical pores, Nature 430 (2004) 764–768, doi:10.1038/nature02770.

[63] V. Percec, A.E. Dulcey, M. Peterca, M. Ilies, S. Nummelin, M.J. Sienkowska, P.A. Heiney, Principles of self-assembly of helical pores from dendritic dipeptides, Proc. Natl. Acad. Sci. U.S.A. 103 (2006) 2518–2523, doi:10.1073/pnas.0509676103.

[64] M.S. Kaucher, M. Peterca, A.E. Dulcey, A.J. Kim, S.A. Vinogradov, D.A. Hammer, P.A. Heiney, V. Percec, Selective transport of water mediated by porous dendritic dipeptides, J. Am. Chem. Soc. 129 (2007) 11698–11699, doi:10.1021/ja076066c.

[65] V. Percec, A.E. Dulcey, M. Peterca, P. Adelman, R. Samant, V.S.K. Balagurusamy, P.A. Heiney, Helical pores self-assembled from homochiral dendritic dipeptides based on L-Tyr and nonpolar alpha-amino acids, J. Am. Chem. Soc. 129 (2007) 5992–6002, doi:10.1021/ja071088k.

[66] V. Percec, J. Smidrkal, M. Peterca, C.M. Mitchell, S. Nummelin, A.E. Dulcey, M.J. Sienkowska, P.A. Heiney, Self-assembly of hybrid dendrons with complex primary structure into functional helical pores, Chem. A Eur. J. 13 (2007) 3989–4007, doi:10.1002/chem.200601582.

[67] M. Peterca, V. Percec, A.E. Dulcey, S. Nummelin, S. Korey, M. Ilies, P.A. Heiney, Self-assembly, structural, and retrostructural analysis of dendritic dipeptide pores undergoing reversible circular to elliptical shape change, J. Am. Chem. Soc. 128 (2006) 6713–6720, doi:10.1021/ja0611902.

[68] B.M. Rosen, M. Peterca, K. Morimitsu, A.E. Dulcey, P. Leowanawat, A.-M. Resmerita, M.R. Imam, V. Percec, Programming the supramolecular helical polymerization of dendritic dipeptides via the stereochemical information of the dipeptide, J. Am. Chem. Soc. 133 (2011) 5135–5151, doi:10.1021/ja200280h.

[69] V. Percec, M. Peterca, A.E. Dulcey, M.R. Imam, S.D. Hudson, S. Nummelin, P. Adelman, P.A. Heiney, Hollow spherical supramolecular dendrimers, J. Am. Chem. Soc. 130 (2008) 13079–13094, doi:10.1021/ja8034703.

[70] V. Percec, A.E. Dulcey, M. Peterca, M. Ilies, J. Ladislaw, B.M. Rosen, U. Edlund, P.A. Heiney, The internal structure of helical pores self-assembled from dendritic dipeptides is stereochemically programmed and allosterically regulated, Angew. Chem. Int. Ed. 44 (2005) 6516–6521, doi:10.1002/anie.200501331.

[71] V. Percec, A. Dulcey, M. Peterca, M. Ilies, Y. Miura, U. Edlund, P.A. Heiney, V. Percec, A. Dulcey, M. Peterca, M. Ilies, Y. Miura, U. Edlund, P.A. Heiney, Helical porous protein mimics self-assembled from amphiphilic dendritic dipeptides, Aust. J. Chem. 58 (2005) 472–482, doi:10.1071/CH05092.

[72] V. Percec, J.G. Rudick, M. Peterca, P.A. Heiney, Nanomechanical function from self-organizable dendronized helical polyphenylacetylenes, J. Am. Chem. Soc. 130 (2008) 7503–7508, doi:10.1021/ja801863e.

[73] V. Percec, M.R. Imam, M. Peterca, P. Leowanawat, Self-organizable vesicular columns assembled from polymers dendronized with semifluorinated Janus

dendrimers act as reverse thermal actuators, J. Am. Chem. Soc. 134 (2012) 4408–4420, doi:10.1021/ja2118267.

[74] K.A. Andreopoulou, M. Peterca, D.A. Wilson, B.E. Partridge, P.A. Heiney, V. Percec, Demonstrating the 8_1-helicity and nanomechanical function of self-organizable dendronized polymethacrylates and polyacrylates, macromolecules 50 (2017) 5271–5284, doi:10.1021/acs.macromol.7b01216.

[75] D. Jishkariani, C.M. MacDermaid, Y.N. Timsina, S. Grama, S.S. Gillani, M. Divar, S.S. Yadavalli, R.-O. Moussodia, P. Leowanawat, A.M.B. Camacho, R. Walter, M. Goulian, M.L. Klein, V. Percec, Self-interrupted synthesis of sterically hindered aliphatic polyamide dendrimers, Proc. Natl. Acad. Sci. U.S.A. 114 (2017) E2275–E2284, doi:10.1073/pnas.1700922114.

[76] V. Percec, C.-H. Ahn, B. Barboiu, Self-encapsulation, acceleration and control in the radical polymerization of monodendritic monomers via self-assembly, J. Am. Chem. Soc. 119 (1997) 12978–12979, doi:10.1021/ja9727878.

[77] V. Percec, C.-H. Ahn, G. Ungar, D.J.P. Yeardley, M. Möller, S.S. Sheiko, Controlling polymer shape through the self-assembly of dendritic side-groups, Nature 391 (1998) 161–164, doi:10.1038/34384.

[78] V. Percec, C.-H. Ahn, W.-D. Cho, A.M. Jamieson, J. Kim, T. Leman, M. Schmidt, M. Gerle, M Möller, S.A. Prokhorova, S.S. Sheiko, S.Z.D. Cheng, A. Zhang, G. Ungar, D.J.P. Yeardley, Visualizable cylindrical macromolecules with controlled stiffness from backbones containing libraries of self-assembling dendritic side groups, J. Am. Chem. Soc. 120 (1998) 8619–8631, doi:10.1021/ja981211v.

[79] M.N. Holerca, M. Peterca, B.E. Partridge, Q. Xiao, G. Lligadas, M.J. Monteiro, V. Percec, Monodisperse macromolecules by self-interrupted living polymerization, J. Am. Chem. Soc. 142 (2020) 15265–15270, doi:10.1021/jacs.0c07912.

[80] V. Percec, J.G. Rudick, M. Peterca, M. Wagner, M. Obata, C.M. Mitchell, W.-D. Cho, V.S.K. Balagurusamy, P.A. Heiney, Thermoreversible cis−cisoidal to cis−transoidal isomerization of helical dendronized polyphenylacetylenes, J. Am. Chem. Soc. 127 (2005) 15257–15264, doi:10.1021/ja055406w.

[81] B.M. Rosen, C. Roche, V. Percec, Self-assembly of dendritic dipeptides as a model of chiral selection in primitive biological systems, Top. Curr. Chem. 333 (2013) 213–253, doi:10.1007/128_2012_398.

[82] C. Roche, H.-J. Sun, M.E. Prendergast, P. Leowanawat, B.E. Partridge, P.A. Heiney, F. Araoka, R. Graf, H.W. Spiess, X. Zeng, G. Ungar, V. Percec, Homochiral columns constructed by chiral self-sorting during supramolecular helical organization of hat-ahaped molecules, J. Am. Chem. Soc. 136 (2014) 7169–7185, doi:10.1021/ja5035107.

[83] C. Roche, H.-J. Sun, P. Leowanawat, F. Araoka, B.E. Partridge, M. Peterca, D.A. Wilson, M.E. Prendergast, P.A. Heiney, R. Graf, H.W. Spiess, X. Zeng, G. Ungar, V. Percec, A supramolecular helix that disregards chirality, Nat. Chem. 8 (2016) 80–89, doi:10.1038/nchem.2397.

[84] B.E. Partridge, L. Wang, D. Sahoo, J.T. Olsen, P. Leowanawat, C. Roche, H. Ferreira, K.J. Reilly, X. Zeng, G. Ungar, P.A. Heiney, R. Graf, H.W. Spiess, V. Percec, Sequence-defined dendrons dictate supramolecular cogwheel assembly of dendronized perylene bisimides, J. Am. Chem. Soc. 141 (2019) 15761–15766, doi:10.1021/jacs.9b08714.

[85] L. Wang, B.E. Partridge, N. Huang, J.T. Olsen, D. Sahoo, X. Zeng, G. Ungar, R. Graf, H.W. Spiess, V. Percec, Extraordinary acceleration of cogwheel helical self-organization of dendronized perylene bisimides by the dendron sequence encoding their tertiary structure, J. Am. Chem. Soc. 142 (2020) 9525–9536, doi:10.1021/jacs.0c03353.

[86] V. Percec, P. Chu, G. Ungar, J. Zhou, Rational design of the first nonspherical dendrimer which displays calamitic nematic and smectic thermotropic liquid crystalline phases, J. Am. Chem. Soc. 117 (1995) 11441–11454, doi:10.1021/ja00151a008.

[87] D.A. Wilson, K.A. Andreopoulou, M. Peterca, P. Leowanawat, D. Sahoo, B.E. Partridge, Q. Xiao, N. Huang, P.A. Heiney, V. Percec, Supramolecular spheres self-assembled from conical dendrons are chiral, J. Am. Chem. Soc. 141 (2019) 6162–6166, doi:10.1021/jacs.9b02206.

[88] D. Sahoo, M.R. Imam, M. Peterca, B.E. Partridge, D.A. Wilson, X. Zeng, G. Ungar, P.A. Heiney, V. Percec, Hierarchical self-organization of chiral columns from chiral supramolecular spheres, J. Am. Chem. Soc. 140 (2018) 13478–13487, doi:10.1021/jacs.8b09174.

[89] V. Percec, M. Lee, Molecular engineering of liquid crystal polymers by living polymerization. XXIII. Synthesis and characterization of AB block copolymers based on ω-[(4-cyano-4′ -biphenyl)-oxy]alkyl vinyl ether, 1H, 1H, 2H, 2H-perfluorodecyl vinyl ether, and 2-(4-biphenyloxy)ethyl vinyl ether with 1H, 1H, 2H, 2H-perfluorodecyl vinyl ether, J. Macromol. Sci., Part A. Pure Appl. Chem. 29 (1992) 723–740, doi:10.1080/10601329208054112.

[90] V. Percec, G. Johansson, G. Ungar, J. Zhou, Fluorophobic effect induces the self-assembly of semifluorinated tapered monodendrons containing crown ethers into supramolecular columnar dendrimers which exhibit a homeotropic hexagonal columnar liquid crystalline phase, J. Am. Chem. Soc. 118 (1996) 9855–9866, doi:10.1021/ja9615738.

[91] V. Percec, M. Glodde, M. Peterca, A. Rapp, I. Schnell, H.W. Spiess, T.K. Bera, Y. Miura, V.S.K. Balagurusamy, E. Aqad, P.A. Heiney, Self-assembly of semifluorinated dendrons attached to electron-donor groups mediates their π-stacking via a helical pyramidal column, Chem. Eur. J. 12 (2006) 6298–6314, doi:10.1002/chem.200501195.

[92] G. Johansson, V. Percec, G. Ungar, J.P. Zhou, Fluorophobic effect in the self-assembly of polymers and model compounds containing tapered groups into supramolecular columns, Macromolecules 29 (1996) 646–660, doi:10.1021/ma9511558.

[93] D.R. Dukeson, G. Ungar, V.S.K. Balagurusamy, V. Percec, G.A. Johansson, M. Glodde, Application of isomorphous replacement in the structure determination of a cubic liquid crystal phase and location of counterions, J. Am. Chem. Soc. 125 (2003) 15974–15980, doi:10.1021/ja037380j.

[94] V. Percec, D. Tomazos, A.E. Feiring, Semifluorinated polymers: 1. Synthesis and characterization of side chain liquid crystalline polymers containing semifluorinated oligooxyethylene based flexible spacers, Polymer 32 (1991) 1897–1908, doi:10.1016/0032-3861(91)90382-S.

[95] G. Johansson, V. Percec, G. Ungar, K. Smith, Fluorophobic effect generates a systematic approach to the synthesis of the simplest class of rodlike liquid crystals containing a single benzene unit, Chem. Mater. 9 (1997) 164–175, doi:10.1021/cm960267q.

[96] V. Percec, E. Aqad, M. Peterca, M.R. Imam, M. Glodde, T.K. Bera, Y. Miura, V.S.K. Balagurusamy, P.C. Ewbank, F. Würthner, P.A. Heiney, Self-assembly of semifluorinated minidendrons attached to electron-acceptor groups into pyramidal columns, Chem. Eur. J. 13 (2007) 3330–3345, doi:10.1002/chem.200600901.

[97] V. Percec, M. Glodde, M. Peterca, A. Rapp, I. Schnell, H.W. Spiess, T.K. Bera, Y. Miura, V.S.K. Balagurusamy, E. Aqad, P.A. Heiney, Self-assembly of semifluorinated dendrons attached to electron-donor groups mediates their π-stacking via a helical pyramidal column, Chem. Eur. J. 12 (2006) 6298–6314, doi:10.1002/chem.200501195.

[98] I. Shiyanovskaya, K.D. Singer, V. Percec, T.K. Bera, Y. Miura, M. Glodde, Charge transport in hexagonal columnar liquid crystals self-organized from supramolecular cylinders based on acene-functionalized dendrons, Phys. Rev. B. 67 (2003) 035204, doi:10.1103/PhysRevB.67.035204.

[99] V. Percec, W.-D. Cho, G. Ungar, D.J.P. Yeardley, Synthesis and structural analysis of two constitutional isomeric libraries of AB_2-based monodendrons and supramolecular dendrimers, J. Am. Chem. Soc. 123 (2001) 1302–1315, doi:10.1021/ja0037771.

[100] V. Percec, C.M. Mitchell, W.-D. Cho, S. Uchida, M. Glodde, G. Ungar, X. Zeng, Y. Liu, V.S.K. Balagurusamy, P.A. Heiney, Designing libraries of first generation AB_3 and AB_2 self-assembling dendrons *via* the primary structure generated from combinations of $(AB)_y-AB_3$ and $(AB)_y-AB_2$ building blocks, J. Am. Chem. Soc. 126 (2004) 6078–6094, doi:10.1021/ja049846j.

[101] V. Percec, M. Peterca, M.J. Sienkowska, M.A. Ilies, E. Aqad, J. Smidrkal, P.A. Heiney, Synthesis and retrostructural analysis of libraries of AB_3 and constitutional isomeric AB_2 phenylpropyl ether-based supramolecular dendrimers, J. Am. Chem. Soc. 128 (2006) 3324–3334, doi:10.1021/ja060062a.

[102] V. Percec, M.N. Holerca, S. Nummelin, J.J. Morrison, M. Glodde, J. Smidrkal, M. Peterca, B.M. Rosen, S. Uchida, V.S.K. Balagurusamy, M.J. Sienkowska, P.A. Heiney, Exploring and expanding the structural diversity of self-assembling dendrons through combinations of AB, constitutional isomeric AB_2, and AB_3 biphenyl-4-methyl ether building blocks, Chem. Eur. J. 12 (2006) 6216–6241, doi:10.1002/chem.200600178.

[103] B.M. Rosen, D.A. Wilson, C.J. Wilson, M. Peterca, B.C. Won, C. Huang, L.R. Lipski, X. Zeng, G. Ungar, P.A. Heiney, V. Percec, Predicting the structure of supramolecular dendrimers via the analysis of libraries of AB_3 and constitutional isomeric AB_2 biphenylpropyl ether self-assembling dendrons, J. Am. Chem. Soc. 131 (2009) 17500–17521, doi:10.1021/ja907882n.

[104] V. Percec, J.G. Rudick, M. Peterca, M.E. Yurchenko, J. Smidrkal, P.A. Heiney, Supramolecular structural diversity among first-generation hybrid dendrimers and twin dendrons, Chem. Eur. J. 14 (2008) 3355–3362, doi:10.1002/chem.200701658.

[105] B.M. Rosen, M. Peterca, C. Huang, X. Zeng, G. Ungar, V. Percec, Deconstruction as a strategy for the design of libraries of self-assembling dendrons, Angew. Chem. Int. Ed. 49 (2010) 7002–7005, doi:10.1002/anie.201002514.

[106] V. Percec, W.-D. Cho, G. Ungar, D.J.P. Yeardley, Synthesis and NaOTf mediated self-assembly of monodendritic crown ethers, Chem. Eur. J. 8 (2002) 2011–2025, doi:10.1002/1521-3765(20020503)8:9⟨2011::AID-CHEM2011⟩3.0.CO;2-3.

[107] V. Percec, T.K. Bera, M. Glodde, Q. Fu, V.S.K. Balagurusamy, P.A. Heiney, Hierarchical self-assembly, coassembly, and self-organization of novel liquid crystalline lattices and superlattices from a twin-tapered dendritic benzamide and its four-cylinder-bundle supramolecular polymer, Chem. Eur. J. 9 (2003) 921–935, doi:10.1002/chem.200390114.

[108] S.D. Hudson, H.-T. Jung, V. Percec, W.-D. Cho, G. Johansson, G. Ungar, V.S.K. Balagurusamy, Direct visualization of individual cylindrical and spherical supramolecular dendrimers, Science 278 (1997) 449–452, doi:10.1126/science.278.5337.449.

[109] M. Peterca, V. Percec, M.R. Imam, P. Leowanawat, K. Morimitsu, P.A. Heiney, Molecular structure of helical supramolecular dendrimers, J. Am. Chem. Soc. 130 (2008) 14840–14852, doi:10.1021/ja806524m.

[110] V. Percec, M. Peterca, T. Tadjiev, X. Zeng, G. Ungar, P. Leowanawat, E. Aqad, M.R. Imam, B.M. Rosen, U. Akbey, R. Graf, S. Sekharan, D. Sebastiani, H.W. Spiess, P.A. Heiney, S.D. Hudson, Self-assembly of dendronized perylene bisimides into complex helical columns, J. Am. Chem. Soc. 133 (2011) 12197–12219, doi:10.1021/ja204366b.

[111] G. Ungar, D. Abramic, V. Percec, J.A. Heck, Self-assembly of twin tapered bisamides into supramolecular columns exhibiting hexagonal columnar mesophases. Structural evidence for a microsegregated model of the supramolecular column, Liq. Cryst. 21 (1996) 73–86, doi:10.1080/02678299608033797.

[112] V. Percec, W.-D. Cho, G. Ungar, Increasing the diameter of cylindrical and spherical supramolecular dendrimers by decreasing the solid angle of their monodendrons *via* periphery functionalization, J. Am. Chem. Soc. 122 (2000) 10273–10281, doi:10.1021/ja0024643.

[113] V. Percec, M.R. Imam, T.K. Bera, V.S.K. Balagurusamy, M. Peterca, P.A. Heiney, Self-assembly of semifluorinated Janus-dendritic benzamides into bilayered pyramidal columns, Angew. Chem. Int. Ed. 44 (2005) 4739–4745, doi:10.1002/anie.200501254.

[114] V. Percec, M. Glodde, G. Johansson, V.S.K. Balagurusamy, P.A. Heiney, Transformation of a spherical supramolecular dendrimer into a pyramidal columnar supramolecular dendrimer mediated by the fluorophobic effect, Angew. Chem. Int. Ed. 42 (2003) 4338–4342, doi:10.1002/anie.200351804.

[115] V. Percec, B.C. Won, M. Peterca, P.A. Heiney, Expanding the structural diversity of self-assembling dendrons and supramolecular dendrimers via complex building blocks, J. Am. Chem. Soc. 129 (2007) 11265–11278, doi:10.1021/ja073714j.

[116] G. Ungar, V. Percec, M.N. Holerca, G. Johansson, J.A. Heck, Heat-shrinking spherical and columnar supramolecular dendrimers: Their interconversion and dependence of their shape on molecular taper angle, Chem. Eur. J. 6 (2000) 1258–1266, doi:10.1002/(SICI)1521-3765(20000403)6:7⟨1258::AID-CHEM1258⟩3.0.CO;2-O.

[117] V. Percec, M.N. Holerca, S. Uchida, W.-D. Cho, G. Ungar, Y. Lee, D.J.P. Yeardley, Exploring and expanding the three-dimensional structural diversity of supramolecular dendrimers with the aid of libraries of alkali metals of their AB_3 minidendritic carboxylates, Chem. Eur. J. 8 (2002) 1106–1117, doi:10.1002/1521-3765(20020301)8:5⟨1106::AID-CHEM1106⟩3.0.CO;2-G.

[118] V. Percec, W.-D. Cho, P.E. Mosier, G. Ungar, D.J.P. Yeardley, Structural analysis of cylindrical and spherical supramolecular dendrimers quantifies the concept of monodendron shape control by generation number, J. Am. Chem. Soc. 120 (1998) 11061–11070, doi:10.1021/ja9819007.

[119] V. Percec, W.-D. Cho, M. Möller, S.A. Prokhorova, G. Ungar, D.J.P. Yeardley, Design and structural analysis of the first spherical monodendron self-organizable in a cubic lattice, J. Am. Chem. Soc. 122 (2000) 4249–4250, doi:10.1021/ja9943400.

[120] D.J.P. Yeardley, G. Ungar, V. Percec, M.N. Holerca, G. Johansson, Spherical Supramolecular minidendrimers self-organized in an "inverse micellar"-like thermotropic body-centered cubic liquid crystalline phase, J. Am. Chem. Soc. 122 (2000) 1684–1689, doi:10.1021/ja993915q.

[121] V. Percec, E. Aqad, M. Peterca, J.G. Rudick, L. Lemon, J.C. Ronda, B.B. De, P.A. Heiney, E.W. Meijer, Steric communication of chiral information observed in dendronized polyacetylenes, J. Am. Chem. Soc. 128 (2006) 16365–16372, doi:10.1021/ja0665848.

[122] V. Percec, C.-H. Ahn, T.K. Bera, G. Ungar, D.J.P. Yeardley, Coassembly of a hexagonal columnar liquid crystalline superlattice from polymer(s) coated with a three-cylindrical bundle supramolecular dendrimer, Chem. Eur. J. 5 (1999) 1070–1083, doi:10.1002/(SICI)1521-3765(19990301)5:3⟨1070::AID-CHEM1070⟩3.0.CO;2-9.

[123] V. Percec, M.N. Holerca, S.N. Magonov, D.J.P. Yeardley, G. Ungar, H. Duan, S.D. Hudson, Poly(oxazolines)s with tapered minidendritic side groups. The simplest cylindrical models to investigate the formation of two-dimensional and three-dimensional order by direct visualization, Biomacromolecules 2 (2001) 706–728, doi:10.1021/bm015550j.

[124] V. Percec, M.N. Holerca, S. Uchida, D.J.P. Yeardley, G. Ungar, Poly(oxazoline)s with tapered minidendritic side groups as models for the design of synthetic macromolecules with tertiary structure. A demonstration of the limitations of living polymerization in the design of 3-D structures based on single polymer chains, Biomacromolecules 2 (2001) 729–740, doi:10.1021/bm015559l.

[125] V. Percec, M.N. Holerca, Detecting the shape change of complex macromolecules during their synthesis with the aid of kinetics. A new lesson from biology, Biomacromolecules 1 (2000) 6–16, doi:10.1021/bm005507g.

[126] M.N. Holerca, D. Sahoo, M. Peterca, B.E. Partridge, P.A. Heiney, V. Percec, A tetragonal phase self-organized from unimolecular spheres assembled from a substituted poly(2-oxazoline), Macromolecules 50 (2017) 375–385, doi:10.1021/acs.macromol.6b02298.

[127] M.N. Holerca, D. Sahoo, B.E. Partridge, M. Peterca, X. Zeng, G. Ungar, V. Percec, Dendronized poly(2-oxazoline) displays within only five monomer repeat units liquid quasicrystal, A15 and σ Frank–Kasper phases, J. Am. Chem. Soc. 140 (2018) 16941–16947, doi:10.1021/jacs.8b11103.

[128] V.S.K. Balagurusamy, G. Ungar, V. Percec, G. Johansson, Rational design of the first spherical supramolecular dendrimers self-organized in a novel thermotropic cubic liquid-crystalline phase and the determination of their shape by X-ray analysis, J. Am. Chem. Soc. 119 (1997) 1539–1555, doi:10.1021/ja963295i.

[129] G. Ungar, Y. Liu, X. Zeng, V. Percec, W.-D. Cho, Giant supramolecular liquid crystal lattice, Science 299 (2003) 1208–1211, doi:10.1126/science.1078849.

[130] M.R. Imam, M. Peterca, U. Edlund, V.S.K. Balagurusamy, V. Percec, Dendronized supramolecular polymers self-assembled from dendritic ionic liquids, J. Polym. Sci. Part A: Polym. Chem. 47 (2009) 4165–4193, doi:10.1002/pola.23523.

[131] V. Percec, W.-D. Cho, G. Ungar, D.J.P. Yeardley, From molecular flat tapers, discs, and cones to supramolecular cylinders and spheres using Fréchet-type monodendrons modified on their leriphery, Angew. Chem. Int. Ed. 39 (2000) 1597–1602, doi:10.1002/(SICI)1521-3773(20000502)39:9⟨1597::AID-ANIE1597⟩3.0.CO;2-I.

[132] A. Rapp, I. Schnell, D. Sebastiani, S.P. Brown, V. Percec, H.W. Spiess, Supramolecular assembly of dendritic polymers elucidated by ^{1}H and ^{13}C solid-state MAS NMR spectroscopy, J. Am. Chem. Soc. 125 (2003) 13284–13297, doi:10.1021/ja035127d.

[133] M. Peterca, M.R. Imam, P. Leowanawat, B.M. Rosen, D.A. Wilson, C.J. Wilson, X. Zeng, G. Ungar, P.A. Heiney, V. Percec, Self-assembly of hybrid dendrons into doubly segregated supramolecular polyhedral columns and vesicles, J. Am. Chem. Soc. 132 (2010) 11288–11305, doi:10.1021/ja104432d.

[134] V. Percec, M. Peterca, Y. Tsuda, B.M. Rosen, S. Uchida, M.R. Imam, G. Ungar, P.A. Heiney, Elucidating the structure of the Pm3n cubic phase of supramolecular dendrimers through the modification of their aliphatic to aromatic volume ratio, Chem. Eur. J. 15 (2009) 8994–9004, doi:10.1002/chem.200901324.

[135] X. Zeng, G. Ungar, Y. Liu, V. Percec, A.E. Dulcey, J.K. Hobbs, Supramolecular dendritic liquid quasicrystals, Nature 428 (2004) 157–160, doi:10.1038/nature02368.

[136] G. Ungar, V. Percec, X. Zeng, P. Leowanawat, Liquid quasicrystals, Isr. J. Chem. 51 (2011) 1206–1215, doi:10.1002/ijch.201100151.

[137] V. Percec, M.R. Imam, M. Peterca, W.-D. Cho, P.A. Heiney, Self-assembling dendronized dendrimers, Isr. J. Chem. 49 (2009) 55–70, doi:10.1560/IJC.49.1.55.

[138] V. Percec, S.D. Hudson, M. Peterca, P. Leowanawat, E. Aqad, R. Graf, H.W. Spiess, X. Zeng, G. Ungar, P.A. Heiney, Self-repairing complex helical columns generated via kinetically controlled self-assembly of dendronized perylene bisimides, J. Am. Chem. Soc. 133 (2011) 18479–18494, doi:10.1021/ja208501d.

[139] V. Percec, S. Wang, N. Huang, B.E. Partridge, X. Wang, D. Sahoo, D.J. Hoffman, J. Malineni, M. Peterca, R.L. Jezorek, N. Zhang, H. Daud, P.D. Sung, E.R. McClure, S.L. Song, An accelerated modular-orthogonal Ni-catalyzed methodology to symmetric and nonsymmetric constitutional isomeric AB_2 to AB_9 dendrons exhibiting unprecedented self-organizing principles, J. Am. Chem. Soc. 143 (2021) 17724–17743, doi:10.1021/jacs.1c08502.

[140] V. Percec, D.A. Wilson, P. Leowanawat, C.J. Wilson, A.D. Hughes, M.S. Kaucher, D.A. Hammer, D.H. Levine, A.J. Kim, F.S. Bates, K.P. Davis, T.P. Lodge, M.L. Klein, R.H. DeVane, E. Aqad, B.M. Rosen, A.O. Argintaru, M.J. Sienkowska, K. Rissanen, S. Nummelin, J. Ropponen, Self-assembly of Janus dendrimers into uniform dendrimersomes and other complex architectures, Science 328 (2010) 1009–1014, doi:10.1126/science.1185547.

[141] M. Peterca, V. Percec, P. Leowanawat, A. Bertin, Predicting the Size and Properties of Dendrimersomes from the Lamellar Structure of Their Amphiphilic Janus Dendrimers, J. Am. Chem. Soc. 133 (2011) 20507–20520, doi:10.1021/ja208762u.

[142] S.E. Sherman, Q. Xiao, V. Percec, Mimicking Complex Biological Membranes and Their Programmable Glycan Ligands with Dendrimersomes and Glycodendrimersomes, Chem. Rev. 117 (2017) 6538–6631, doi:10.1021/acs.chemrev.7b00097.

[143] S. Zhang, H.-J. Sun, A.D. Hughes, B. Draghici, J. Lejnieks, P. Leowanawat, A. Bertin, L. Otero De Leon, O.V. Kulikov, Y. Chen, D.J. Pochan, P.A. Heiney, V. Percec, Single–Single" Amphiphilic Janus Dendrimers Self-Assemble into Uniform Dendrimersomes with Predictable Size, ACS Nano 8 (2014) 1554–1565, doi:10.1021/nn405790x.

[144] S. Zhang, H.-J. Sun, A.D. Hughes, R.-O. Moussodia, A. Bertin, Y. Chen, D.J. Pochan, P.A. Heiney, M.L. Klein, V. Percec, Self-assembly of amphiphilic Janus dendrimers into uniform onion-like dendrimersomes with predictable size and number of bilayers, Proc Natl Acad Sci U S A 111 (2014) 9058–9063, doi:10.1073/pnas.1402858111.

[145] Q. Xiao, J.D. Rubien, Z. Wang, E.H. Reed, D.A. Hammer, D. Sahoo, P.A. Heiney, S.S. Yadavalli, M. Goulian, S.E. Wilner, T. Baumgart, S.A. Vinogradov, M.L. Klein, V. Percec, Self-Sorting and Coassembly of Fluorinated, Hydrogenated, and Hybrid Janus Dendrimers into Dendrimersomes, J. Am. Chem. Soc. 138 (2016) 12655–12663, doi:10.1021/jacs.6b08069.

[146] Q. Xiao, S.S. Yadavalli, S. Zhang, S.E. Sherman, E. Fiorin, L. da Silva, D.A. Wilson, D.A. Hammer, S. André, H.-J. Gabius, M.L. Klein, M. Goulian, V. Percec, Bioactive cell-like hybrids coassembled from (glyco)dendrimersomes with bacterial membranes, Proc Natl Acad Sci U S A 113 (2016) E1134–E1141, doi:10.1073/pnas.1525589113.

[147] Q. Xiao, S.E. Sherman, S.E. Wilner, X. Zhou, C. Dazen, T. Baumgart, E.H. Reed, D.A. Hammer, W. Shinoda, M.L. Klein, V. Percec, Janus dendrimersomes coassembled from fluorinated, hydrogenated, and hybrid Janus dendrimers as models for cell fusion and fission, Proc Natl Acad Sci U S A 114 (2017) E7045–E7053, doi:10.1073/pnas.1708380114.

[148] P. Torre, Q. Xiao, I. Buzzacchera, S.E. Sherman, K. Rahimi, N.Y. Kostina, C. Rodriguez-Emmenegger, M. Möller, C.J. Wilson, M.L. Klein, M.C. Good, V. Percec, Encapsulation of hydrophobic components in dendrimersomes and

decoration of their surface with proteins and nucleic acids, Proc Natl Acad Sci U S A. 116 (2019) 15378–15385, doi:10.1073/pnas.1904868116.

[149] S.S. Yadavalli, Q. Xiao, S.E. Sherman, W.D. Hasley, M.L. Klein, M. Goulian, V. Percec, Bioactive cell-like hybrids from dendrimersomes with a human cell membrane and its components, Proc Natl Acad Sci U S A. 116 (2019) 744–752, doi:10.1073/pnas.1811307116.

[150] I. Buzzacchera, Q. Xiao, H. Han, K. Rahimi, S. Li, N.Yu. Kostina, B.J. Toebes, S.E. Wilner, M. Möller, C. Rodriguez-Emmenegger, T. Baumgart, D.A. Wilson, C.J. Wilson, M.L. Klein, V. Percec, Screening Libraries of Amphiphilic Janus Dendrimers Based on Natural Phenolic Acids to Discover Monodisperse Unilamellar Dendrimersomes, Biomacromolecules 20 (2019) 712–727, doi:10.1021/acs.biomac.8b01405.

[151] N.Yu. Kostina, K. Rahimi, Q. Xiao, T. Haraszti, S. Dedisch, J.P. Spatz, U. Schwaneberg, M.L. Klein, V. Percec, M. Möller, C. Rodriguez-Emmenegger, Membrane-Mimetic Dendrimersomes Engulf Living Bacteria via Endocytosis, Nano Lett 19 (2019) 5732–5738, doi:10.1021/acs.nanolett.9b02349.

[152] S. Li, B. Xia, B. Javed, W.D. Hasley, A. Melendez-Davila, M. Liu, M. Kerzner, S. Agarwal, Q. Xiao, P. Torre, J.G. Bermudez, K. Rahimi, N.Yu. Kostina, M. Möller, C. Rodriguez-Emmenegger, M.L. Klein, V. Percec, M.C. Good, Direct Visualization of Vesicle Disassembly and Reassembly Using Photocleavable Dendrimers Elucidates Cargo Release Mechanisms, ACS Nano 14 (2020) 7398–7411, doi:10.1021/acsnano.0c02912.

[153] N.Y. Kostina, A.M. Wagner, T. Haraszti, K. Rahimi, Q. Xiao, M.L. Klein, V. Percec, C. Rodriguez-Emmenegger, Unraveling topology-induced shape transformations in dendrimersomes, Soft Matter 17 (2021) 254–267, doi:10.1039/D0SM01097A.

[154] V. Percec, P. Leowanawat, H.-J. Sun, O. Kulikov, C.D. Nusbaum, T.M. Tran, A. Bertin, D.A. Wilson, M. Peterca, S. Zhang, N.P. Kamat, K. Vargo, D. Moock, E.D. Johnston, D.A. Hammer, D.J. Pochan, Y. Chen, Y.M. Chabre, T.C. Shiao, M. Bergeron-Brlek, S. André, R. Roy, H.-J. Gabius, P.A. Heiney, Modular Synthesis of Amphiphilic Janus Glycodendrimers and Their Self-Assembly into Glycodendrimersomes and Other Complex Architectures with Bioactivity to Biomedically Relevant Lectins, J. Am. Chem. Soc. 135 (2013) 9055–9077, doi:10.1021/ja403323y.

[155] S. Zhang, Q. Xiao, S.E. Sherman, A. Muncan, A.D.M. Ramos Vicente, Z. Wang, D.A. Hammer, D. Williams, Y. Chen, D.J. Pochan, S. Vértesy, S. André, M.L. Klein, H.-J. Gabius, V. Percec, Glycodendrimersomes from Sequence-Defined Janus Glycodendrimers Reveal High Activity and Sensor Capacity for the Agglutination by Natural Variants of Human Lectins, J. Am. Chem. Soc. 137 (2015) 13334–13344, doi:10.1021/jacs.5b08844.

[156] Q. Xiao, S. Zhang, Z. Wang, S.E. Sherman, R.-O. Moussodia, M. Peterca, A. Muncan, D.R. Williams, D.A. Hammer, S. Vértesy, S. André, H.-J. Gabius, M.L. Klein, V. Percec, Onion-like glycodendrimersomes from sequence-defined Janus glycodendrimers and influence of architecture on reactivity to a lectin, Proc Natl Acad Sci U S A 113 (2016) 1162–1167, doi:10.1073/pnas.1524976113.

[157] Q. Xiao, Z. Wang, D. Williams, P. Leowanawat, M. Peterca, S.E. Sherman, S. Zhang, D.A. Hammer, P.A. Heiney, S.R. King, D.M. Markovitz, S. André, H.-J. Gabius, M.L. Klein, V. Percec, Why Do Membranes of Some Unhealthy Cells Adopt a Cubic Architecture? ACS Cent. Sci. (2016), doi:10.1021/acscentsci.6b00284.

[158] Q. Xiao, A.-K. Ludwig, C. Romanò, I. Buzzacchera, S.E. Sherman, M. Vetro, S. Vértesy, H. Kaltner, E.H. Reed, M. Möller, C.J. Wilson, D.A. Hammer, S. Oscarson, M.L. Klein, H.-J. Gabius, V. Percec, Exploring functional pairing between surface glycoconjugates and human galectins using programmable glycodendrimersomes, Proc Natl Acad Sci U S A 115 (2018) E2509–E2518, doi:10.1073/pnas.1720055115.

[159] C. Rodriguez-Emmenegger, Q. Xiao, N.Y. Kostina, S.E. Sherman, K. Rahimi, B.E. Partridge, S. Li, D. Sahoo, A.M.R. Perez, I. Buzzacchera, H. Han, M. Kerzner, I. Malhotra, M. Möller, C.J. Wilson, M.C. Good, M. Goulian, T. Baumgart, M.L. Klein, V. Percec, Encoding biological recognition in a bicomponent cell-membrane mimic, Proc Natl Acad Sci U S A. (2019) 201821924, doi:10.1073/pnas.1821924116.

[160] Q. Xiao, M. Delbianco, S.E. Sherman, A.M.R. Perez, P. Bharate, A. Pardo-Vargas, C. Rodriguez-Emmenegger, N.Y. Kostina, K. Rahimi, D. Söder, M. Möller, M.L. Klein, P.H. Seeberger, V. Percec, Nanovesicles displaying functional linear and branched oligomannose self-assembled from sequence-defined Janus glycodendrimers, Proc Natl Acad Sci U S A 117 (2020) 11931–11939, doi:10.1073/pnas.2003938117.

[161] P.V. Murphy, A. Romero, Q. Xiao, A.-K. Ludwig, S. Jogula, N.V. Shilova, T. Singh, A. Gabba, B. Javed, D. Zhang, F.J. Medrano, H. Kaltner, J. Kopitz, N.V. Bovin, A.M. Wu, M.L. Klein, V. Percec, H.-J. Gabius, Probing sulfatide-tissue lectin recognition with functionalized glycodendrimersomes, iScience 24 (2021) 101919, doi:10.1016/j.isci.2020.101919.

[162] N.Y. Kostina, D. Söder, T. Haraszti, Q. Xiao, K. Rahimi, B.E. Partridge, M.L. Klein, V. Percec, C. Rodriguez-Emmenegger, Enhanced Concanavalin A Binding to Preorganized Mannose Nanoarrays in Glycodendrimersomes Revealed Multivalent Interactions, Angew Chem Int Ed 60 (2021) 8352–8360, doi:10.1002/anie.202100400.

[163] Q. Xiao, N. Rivera-Martinez, C.J. Raab, J.G. Bermudez, M.C. Good, M.L. Klein, V. Percec, Co-assembly of liposomes, dendrimersomes, and polymersomes with amphiphilic Janus dendrimers conjugated to mono- and tris-nitrilotriacetic acid (NTA, TrisNTA) enhances protein recruitment, Giant 9 (2022) 100089, doi:10.1016/j.giant.2021.100089.

[164] D. Zhang, E.N. Atochina-Vasserman, D.S. Maurya, N. Huang, Q. Xiao, N. Ona, M. Liu, H. Shahnawaz, H. Ni, K. Kim, M.M. Billingsley, D.J. Pochan, M.J. Mitchell, D. Weissman, V. Percec, One-Component Multifunctional Sequence-Defined Ionizable Amphiphilic Janus Dendrimer Delivery Systems for mRNA, J. Am. Chem. Soc. 143 (2021) 12315–12327, doi:10.1021/jacs.1c05813.

[165] D. Zhang, E.N. Atochina-Vasserman, D.S. Maurya, M. Liu, Q. Xiao, J. Lu, G. Lauri, N. Ona, E.K. Reagan, H. Ni, D. Weissman, V. Percec, Targeted Delivery of mRNA with One-Component Ionizable Amphiphilic Janus Dendrimers, J. Am. Chem. Soc. 143 (2021) 17975–17982, doi:10.1021/jacs.1c09585.

[166] D. Zhang, E.N. Atochina-Vasserman, J. Lu, D.S. Maurya, Q. Xiao, M. Liu, J. Adamson, N. Ona, E.K. Reagan, H. Ni, D. Weissman, V. Percec, The Unexpected Importance of the Primary Structure of the Hydrophobic Part of One-Component Ionizable Amphiphilic Janus Dendrimers in Targeted mRNA Delivery Activity, J. Am. Chem. Soc. 144 (2022) 4746–4753, doi:10.1021/jacs.2c00273.

[167] R. Deschenaux, B. Donnio, D. Guillon, Liquid-crystalline fullerodendrimers, New J. Chem. 31 (2007) 1064–1073, doi:10.1039/B617671M.

[168] B. Donnio, S. Buathong, I. Bury, D. Guillon, Liquid crystalline dendrimers, Chem. Soc. Rev. 36 (2007) 1495–1513, doi:10.1039/B605531C.

[169] D. Guillon, R. Deschenaux, Liquid-crystalline dendrimers, Curr. Opin. Solid State Mater. Sci. 6 (2002) 515–525, doi:10.1016/S1359-0286(03)00012-3.

[170] B. Donnio, D. Guillon, Liquid crystalline dendrimers and polypedes, Adv. Polym. Sci. 201 (2006) 45–155, doi:10.1007/12_079.

[171] J.-F. Nierengarten, Chemical modification of C_{60} for materials science applications, New J. Chem. 28 (2004) 1177–1191, doi:10.1039/B402661F.

[172] M. Peterca, M.R. Imam, S.D. Hudson, B.E. Partridge, D. Sahoo, P.A. Heiney, M.L. Klein, V. Percec, Complex arrangement of orthogonal nanoscale columns via a supramolecular orientational memory effect, ACS Nano 10 (2016) 10480–10488, doi:10.1021/acsnano.6b06419.

[173] D. Sahoo, M. Peterca, E. Aqad, B.E. Partridge, P.A. Heiney, R. Graf, H.W. Spiess, X. Zeng, V. Percec, Tetrahedral arrangements of perylene bisimide columns via supramolecular orientational memory, ACS Nano 11 (2017) 983–991, doi:10.1021/acsnano.6b07599.

[174] D. Sahoo, M. Peterca, E. Aqad, B.E. Partridge, M.L. Klein, V. Percec, Losing supramolecular orientational memory via self-organization of a misfolded secondary structure, Polym. Chem. 9 (2018) 2370–2381, doi:10.1039/C8PY00187A.

[175] N. Huang, M.R. Imam, M.J. Sienkowska, M. Peterca, M.N. Holerca, D.A. Wilson, B.M. Rosen, B.E. Partridge, Q. Xiao, V. Percec, Supramolecular spheres assembled from covalent and supramolecular dendritic crowns dictate the supramolecular orientational memory effect mediated by Frank-Kasper phases, Giant 1 (2020) 100001, doi:10.1016/j.giant.2020.100001.

[176] N. Huang, Q. Xiao, M. Peterca, X. Zeng, V. Percec, Self-Organisation of rhombitruncated cuboctahedral hexagonal columns from an amphiphilic Janus dendrimer, Mol. Phys. 119 (2021) e1902586, doi:10.1080/00268976.2021.1902586.

[177] V. Percec, N. Huang, Q. Xiao, B.E. Partridge, D. Sahoo, M.R. Imam, M. Peterca, R. Graf, H.-W. Spiess, X. Zeng, G. Ungar, Self-organization of rectangular bipyramidal helical columns by supramolecular orientational memory epitaxially nucleated from a Frank-Kasper σ phase, Giant 9 (2022) 100084, doi:10.1016/j.giant.2021.100084.

[178] D. Sahoo, M. Peterca, M.R. Imam, B.E. Partridge, Q. Xiao, V. Percec, Conformationally flexible dendronized cyclotetraveratrylenes (CTTVs) self-organize a large diversity of chiral columnar, Frank-Kasper and quasicrystal phases, Giant (2022) 100096, doi:10.1016/j.giant.2022.100096.

[179] M. Bastos, T. Silva, V. Teixeira, K. Nazmi, J.G.M. Bolscher, S.S. Funari, D. Uhríková, Lactoferrin-Derived antimicrobial peptide induces a micellar cubic phase in a model membrane system, Biophys. J. 101 (2011) L20–L22, doi:10.1016/j.bpj.2011.06.038.

[180] H. Delacroix, T. Gulik-Krzywicki, P. Mariani, V. Luzzati, Freeze-fracture electron microscope study of lipid systems: The cubic phase of space group Pm3n, J. Mol. Biol. 229 (1993) 526–539, doi:10.1006/jmbi.1993.1052.

[181] S. Lee, M.J. Bluemle, F.S. Bates, Discovery of a Frank-Kasper σ phase in sphere-forming block copolymer melts, Science 330 (2010) 349–353, doi:10.1126/science.1195552.

[182] S. Fischer, A. Exner, K. Zielske, J. Perlich, S. Deloudi, W. Steurer, P. Lindner, S Förster, Colloidal quasicrystals with 12-fold and 18-fold diffraction symmetry, Proc. Natl. Acad. Sci. U. S. A. 108 (2011) 1810–1814, doi:10.1073/pnas.1008695108.

[183] J. Zhang, F.S. Bates, Dodecagonal quasicrystalline morphology in a poly(styrene-b-isoprene-b-styrene-b-ethylene oxide) tetrablock terpolymer, J. Am. Chem. Soc. 134 (2012) 7636–7639, doi:10.1021/ja301770v.

[184] T.M. Gillard, S. Lee, F.S. Bates, Dodecagonal quasicrystalline order in a diblock copolymer melt, Proc. Natl. Acad. Sci. U.S.A. 113 (2016) 5167–5172, doi:10.1073/pnas.1601692113.

[185] K. Kim, M.W. Schulze, A. Arora, R.M. Lewis, M.A. Hillmyer, K.D. Dorfman, F.S. Bates, Thermal processing of diblock copolymer melts mimics metallurgy, Science 356 (2017) 520–523, doi:10.1126/science.aam7212.

[186] Y. Sun, R. Tan, Z. Ma, Z. Gan, G. Li, D. Zhou, Y. Shao, W.-B. Zhang, R. Zhang, X.-H. Dong, Discrete block copolymers with diverse architectures: resolving complex spherical phases with one monomer resolution, ACS Cent. Sci. 6 (2020) 1386–1393, doi:10.1021/acscentsci.0c00798.

[187] D.V. Perroni, M.K. Mahanthappa, Inverse *Pmn*, cubic micellar lyotropic phases from zwitterionic triazolium gemini surfactants, Soft Matter 9 (2013) 7919–7922, doi:10.1039/C3SM51238J.

[188] S.A. Kim, K.-J. Jeong, A. Yethiraj, M.K. Mahanthappa, Low-symmetry sphere packings of simple surfactant micelles induced by ionic sphericity, Proc. Natl. Acad. Sci. U.S.A. 114 (2017) 4072–4077, doi:10.1073/pnas.1701608114.

[189] C.M. Baez-Cotto, M.K. Mahanthappa, Micellar mimicry of intermetallic C14 and C15 laves phases by aqueous lyotropic self-assembly, ACS Nano 12 (2018) 3226–3234, doi:10.1021/acsnano.7b07475.

[190] A. Jayaraman, D.Y. Zhang, B.L. Dewing, M.K. Mahanthappa, Path-dependent preparation of complex micelle packings of a hydrated diblock oligomer, ACS Cent. Sci. 5 (2019) 619–628, doi:10.1021/acscentsci.8b00903.

[191] M. Huang, C.-H. Hsu, J. Wang, S. Mei, X. Dong, Y. Li, M. Li, H. Liu, W. Zhang, T. Aida, W.-B. Zhang, K. Yue, S.Z.D. Cheng, Selective assemblies of giant tetrahedra via precisely controlled positional interactions, Science 348 (2015) 424–428, doi:10.1126/science.aaa2421.

[192] K. Yue, M. Huang, R.L. Marson, J. He, J. Huang, Z. Zhou, J. Wang, C. Liu, X. Yan, K. Wu, Z. Guo, H. Liu, W. Zhang, P. Ni, C. Wesdemiotis, W.-B. Zhang, S.C. Glotzer, S.Z.D. Cheng, Geometry induced sequence of nanoscale Frank–Kasper and quasicrystal mesophases in giant surfactants, Proc. Natl. Acad. Sci. U.S.A. 113 (2016) 14195–14200, doi:10.1073/pnas.1609422113.

[193] X. Feng, R. Zhang, Y. Li, Y. Hong, D. Guo, K. Lang, K.-Y. Wu, M. Huang, J. Mao, C. Wesdemiotis, Y. Nishiyama, W. Zhang, W. Zhang, T. Miyoshi, T. Li, S.Z.D. Cheng, Hierarchical self-organization of AB_n dendron-like molecules into a supramolecular lattice sequence, ACS Cent. Sci. 3 (2017) 860–867, doi:10.1021/acscentsci.7b00188.

[194] X. Feng, R. Zhang, Y. Li, Y. Hong, D. Guo, K. Lang, K.-Y. Wu, M. Huang, J. Mao, C. Wesdemiotis, Y. Nishiyama, W. Zhang, W. Zhang, T. Miyoshi, T. Li, S.Z.D. Cheng, Hierarchical self-organization of AB_n dendron-like molecules into a supramolecular lattice sequence, ACS Cent. Sci. 3 (2017) 860–867, doi:10.1021/acscentsci.7b00188.

[195] Z. Su, C.-H. Hsu, Z. Gong, X. Feng, J. Huang, R. Zhang, Y. Wang, J. Mao, C. Wesdemiotis, T. Li, S. Seifert, W. Zhang, T. Aida, M. Huang, S.Z.D. Cheng, Identification of a Frank–Kasper Z phase from shape amphiphile self-assembly, Nat. Chem. 11 (2019) 899–905, doi:10.1038/s41557-019-0330-x.

[196] Y. Liu, T. Liu, X. Yan, Q.-Y. Guo, J. Wang, R. Zhang, S. Zhang, Z. Su, J. Huang, G.-X. Liu, W. Zhang, W. Zhang, T. Aida, K. Yue, M. Huang, S.Z.D. Cheng, Mesoatom alloys *via* self-sorting approach of giant molecules blends, Giant 4 (2020) 100031, doi:10.1016/j.giant.2020.100031.

[197] Y. Liu, T. Liu, X.-Y. Yan, Q.-Y. Guo, H. Lei, Z. Huang, R. Zhang, Y. Wang, J. Wang, F. Liu, F.-G. Bian, E.W. Meijer, T. Aida, M. Huang, S.Z.D. Cheng, Expanding quasiperiodicity in soft matter: Supramolecular decagonal quasicrystals by binary giant molecule blends, Proc. Nalt. Acad. Sci. U.S.A. 119 (2022), doi:10.1073/pnas.2115304119.

[198] G.C. Shearman, A.I.I. Tyler, N.J. Brooks, R.H. Templer, O. Ces, R.V. Law, J.M. Seddon, Ordered micellar and inverse micellar lyotropic phases, Liquid Crystals 37 (2010) 679–694, doi:10.1080/02678292.2010.484917.

[199] D.V. Talapin, E.V. Shevchenko, M.I. Bodnarchuk, X. Ye, J. Chen, C.B. Murray, Quasicrystalline order in self-assembled binary nanoparticle superlattices, Nature 461 (2009) 964–967, doi:10.1038/nature08439.

[200] X. Ye, J. Chen, M. Eric Irrgang, M. Engel, A. Dong, S.C. Glotzer, C.B. Murray, Quasicrystalline nanocrystal superlattice with partial matching rules, Nat. Mater. 16 (2016) 214–219, doi:10.1038/nmat4759.

[201] M. Girard, S. Wang, J.S. Du, A. Das, Z. Huang, V.P. Dravid, B. Lee, C.A. Mirkin, M.O. de la Cruz, Particle analogs of electrons in colloidal crystals, Science 364 (2019) 1174–1178, doi:10.1126/science.aaw8237.

[202] K.K. Lachmayr, C.M. Wentz, L.R. Sita, An exceptionally stable and scalable sugar–polyolefin Frank–Kasper A15 phase, Angew. Chem. Int. Ed. 59 (2020) 1521–1526, doi:10.1002/anie.201912648.

[203] K.K. Lachmayr, L.R. Sita, Small-molecule modulation of soft-matter Frank-Kasper phases: A method for adding function to form, Angew. Chem. Int. Ed. 59 (2020) 3563–3567, doi:10.1002/anie.201915416.

[204] X. Feng, C.J. Burke, M. Zhuo, H. Guo, K. Yang, A. Reddy, I. Prasad, R.-M. Ho, A. Avgeropoulos, G.M. Grason, E.L. Thomas, Seeing mesoatomic distortions in soft-matter crystals of a double-gyroid block copolymer, Nature 575 (2019) 175–179, doi:10.1038/s41586-019-1706-1.

[205] D. Adam, P. Schuhmacher, J. Simmerer, L. Häussling, K. Siemensmeyer, K.H. Etzbachi, H. Ringsdorf, D. Haarer, Fast photoconduction in the highly ordered columnar phase of a discotic liquid crystal, Nature 371 (1994) 141–143, doi:10.1038/371141a0.

[206] C.I. Simionescu, V. Percec, S. Dumitrescu, Polymerization of acetylenic derivatives. XXX. Isomers of polyphenylacetylene, J. Polym. Sci: Polym. Chem. Ed. 15 (1977) 2497–2509, doi:10.1002/pol.1977.170151018.

[207] C.I. Simionescu, V. Percec, Polyarylacetylenes: Structure and properties, J. Polym. Sci: Polym. Symp. 67 (1980) 43–71, doi:10.1002/polc.5070670105.

[208] L.-B. Huang, M. Di Vincenzo, Y. Li, M. Barboiu, Artificial water channels: towards biomimetic membranes for desalination, Chem. Eur. J. 27 (2021) 2224–2239, doi:10.1002/chem.202003470.

[209] Y. Chen, H.-Y. Chang, M.-T. Lee, Z.-R. Yang, C.-H. Wang, K.-Y. Wu, W.-T. Chuang, C.-L. Wang, Dual-axis alignment of bulk artificial water channels by directional water-induced self-assembly, J. Am. Chem. Soc. (2022), doi:10.1021/jacs.2c00929.

[210] P.A. Heiney, Datasqueeze: A software tool for powder and small-angle X-ray diffraction analysis, Comm. Powder Diffr. Newsl. 32 (2005) 9–11.

[211] C.-L. Wang, W.-B. Zhang, H.-J. Sun, R.M. Van Horn, R.R. Kulkarni, C.-C. Tsai, C.-S. Hsu, B. Lotz, X. Gong, S.Z.D. Cheng, A supramolecular "double-cable" structure with a 129_{44} helix in a columnar porphyrin-C_{60} dyad and its application in polymer solar cells, Adv. Energy Mater. 2 (2012) 1375–1382, doi:10.1002/aenm.201200060.

[212] Y. Cao, C. Feng, A. Jakli, C. Zhu, F. Liu, Deciphering chiral structures in soft materials via resonant soft and tender X-ray scattering, Giant 2 (2020) 100018, doi:10.1016/j.giant.2020.100018.

[213] K. Gu, W. Yang, T. Wen, Q. Wang, W. Zhang, M. Han, Z. Shen, X. Fan, R.-M. Ho, Co-assembled twisted superstructures formed by disc-bent core amphiphiles, Giant 9 (2022) 100087, doi:10.1016/j.giant.2021.100087.

[214] M.R. Imam, M. Peterca, Q. Xiao, V. Percec, Enhancing conformational flexibility of dendronized triphenylene via diethylene glycol linkers lowers transitions of helical columnar, Frank-Kasper, and quasicrystal phases, Giant 10 (2022) 100098, doi:10.1016/j.giant.2022.100098.

[215] M.-H. Kwok, C.A. Bohannon, R. Li, B. Zhao, L. Zhu, Ordered hexagonal columnar liquid crystalline self-assembly of mesogen-free sulfonylated side-chain chiral polyethers and their high dielectric property, Giant 8 (2021) 100079, doi:10.1016/j.giant.2021.100079.

[216] W.-J. Li, X.-Q. Wang, W. Wang, Z. Hu, Y. Ke, H. Jiang, C. He, X. Wang, Y.-X. Hu, P.-P. Jia, P. Yin, J. Chen, H. Sun, Z. Sun, L. Xu, H.-B. Yang, Dynamic artificial light-harvesting systems based on rotaxane dendrimers, Giant 2 (2020) 100020, doi:10.1016/j.giant.2020.100020.

[217] J. Luo, X. Sun, J.-F. Yin, P. Yin, T. Liu, Supramolecular Nanostructures Constructed from Cluster-based Hybrid Macromolecules, Giant 2 (2020) 100013, doi:10.1016/j.giant.2020.100013.

[218] L. Yang, N. Su, J. Huang, X. Dou, C. Zhao, C. Feng, Chiral helical supramolecular hydrogels with adjustable pitch and diameter towards high-performance chiroptical detecting, Giant 8 (2021) 100077, doi:10.1016/j.giant.2021.100077.

[219] S. Zhang, E. Beach, P.T. Anastas, L.D. Pfefferle, C.O. Osuji, Self-assembly of supramolecular complexes of charged conjugated polymers and imidazolium-based ionic liquid crystals, Giant 9 (2022) 100088, doi:10.1016/j.giant.2021.100088.

[220] W.-B. Zhang, S.Z.D. Cheng, Giant is different: Size effects and the nature of macromolecules, Giant 1 (2020) 100011, doi:10.1016/j.giant.2020.100011.

[221] S. Herbst, B. Soberats, P. Leowanawat, M. Lehmann, F. Würthner, A Columnar Liquid-Crystal Phase Formed by Hydrogen-Bonded Perylene Bisimide J-Aggregates, Angewandte Chemie International Edition 56 (2017) 2162–2165, doi:10.1002/anie.201612047.

[222] M. Lehmann, M. Dechant, M. Holzapfel, A. Schmiedel, C. Lambert, Fullerene-Filled Liquid-Crystal Stars: A supramolecular click mechanism for the generation of tailored donor-acceptor assemblies, Angew. Chem. Int. Ed. 58 (2019) 3610–3615, doi:10.1002/anie.201812465.

[223] X. Liu, Z. Shi, M. Xie, J. Xu, Z. Zhou, S. Jung, G. Cui, Y. Zuo, T. Li, C. Yu, Z. Liu, S. Zhang, Single-handed double helix and spiral platelet formed by racemate of dissymmetric cages, Angew. Chem. Int. Ed. 60 (2021) 15080–15086, doi:10.1002/anie.202103821.

[224] M.L. Nguyen, J. Byun, S. Kim, J.W. Hyun, K. Hur, T.J. Shin, B.-K. Cho, Ferroelectrically switching helical columnar assembly comprising cisoid conformers of a 1,2,3-triazole-based liquid crystal, Angew. Chem. Int. Ed. 58 (2019) 2749–2753, doi:10.1002/anie.201813195.

[225] A. Alenaizan, C.H. Borca, S.C. Karunakaran, A.K. Kendall, G. Stubbs, G.B. Schuster, C.D. Sherrill, N.V. Hud, X-ray fiber diffraction and computational analyses of stacked hexads in supramolecular polymers: Insight into self-assembly in water by prospective prebiotic nucleobases, J. Am. Chem. Soc. 143 (2021) 6079–6094, doi:10.1021/jacs.0c12010.

[226] A. Maity, M. Gangopadhyay, A. Basu, S. Aute, S.S. Babu, A. Das, Counteranion driven homochiral assembly of a cationic C_3-symmetric gelator through ion-pair assisted hydrogen bond, J. Am. Chem. Soc. 138 (2016) 11113–11116, doi:10.1021/jacs.6b06312.

[227] S. Okuda, N. Ousaka, T. Iwata, R. Ishida, A. Urushima, N. Suzuki, S. Nagano, T. Ikai, E. Yashima, Supramolecular helical assemblies of dirhodium(II) paddlewheels with 1,4-diazabicyclo[2.2.2]octane: A remarkable substituent effect on the helical sense preference and amplification of the helical handedness excess of metallo-supramolecular helical polymers, J. Am. Chem. Soc. 144 (2022) 2775–2792, doi:10.1021/jacs.1c12652.

[228] G.B. Schuster, B.J. Cafferty, S.C. Karunakaran, N.V. Hud, Water-soluble supramolecular polymers of paired and stacked heterocycles: Assembly, structure, properties, and a possible path to pre-RNA, J. Am. Chem. Soc. 143 (2021) 9279–9296, doi:10.1021/jacs.0c13081.

[229] S. Herbst, B. Soberats, P. Leowanawat, M. Stolte, M. Lehmann, F. Würthner, Self-assembly of multi-stranded perylene dye J-aggregates in columnar liquid-crystalline phases, Nat. Commun. 9 (2018) 2646, doi:10.1038/s41467-018-05018-6.

[230] Y. Wang, Y. He, Z. Yu, J. Gao, S. ten Brinck, C. Slebodnick, G.B. Fahs, C.J. Zanelotti, M. Hegde, R.B. Moore, B. Ensing, T.J. Dingemans, R. Qiao, L.A. Madsen, Double helical conformation and extreme rigidity in a rodlike polyelectrolyte, Nat. Commun. 10 (2019) 801, doi:10.1038/s41467-019-08756-3.

[231] Y. Cao, M. Alaasar, A. Nallapaneni, M. Salamończyk, P. Marinko, E. Gorecka, C. Tschierske, F. Liu, N. Vaupotič, C. Zhu, Molecular packing in double gyroid cubic phases revealed via resonant soft X-ray scattering, Phys. Rev. Lett. 125 (2020) 027801, doi:10.1103/PhysRevLett.125.027801.